Structural Biology and Molecular Biophysics
Neuroscience

Direct modulation of TRPM8 ion channels by rapamycin and analog macrolide immunosuppressants

Reviewed Preprint
v2 • February 28, 2025
Revised by authors

Reviewed Preprint
v1 • May 9, 2024

Balázs István Tóth, Bahar Bazeli, Annelies Janssens, Erika Lisztes, Márk Racskó, Balázs Kelemen, Mihály Herczeg, Tamás Milán Nagy, Katalin E Kövér, Argha Mitra, Attila Borics, Tamás Bíró, Thomas Voets

Laboratory of Cellular and Molecular Physiology, Department of Physiology, Faculty of Medicine, University of Debrecen, Debrecen, Hungary • Laboratory of Ion Channel Research, Department of Cellular and Molecular Medicine, KU Leuven, Leuven, Belgium • VIB Center for Brain & Disease Research, Leuven, Belgium • Doctoral School of Molecular Medicine, Faculty of Medicine, University of Debrecen, Debrecen, Hungary • Department of Pharmaceutical Chemistry, University of Debrecen, Debrecen, Hungary • MTA-DE Molecular Recognition and Interaction Research Group, University of Debrecen, Debrecen, Hungary • Department of Chemistry, University of Umeå, Umeå, Sweden • Department of Inorganic and Analytical Chemistry, University of Debrecen, Debrecen, Hungary • Laboratory of Chemical Biology, Institute of Biochemistry, HUN-REN Biological Research Centre, Szeged, Hungary • Theoretical Medicine Doctoral School, Faculty of Medicine, University of Szeged, Szeged, Hungary • Department of Immunology, Faculty of Medicine, University of Debrecen, Debrecen, Hungary

eLife Assessment

This manuscript presents **valuable** findings showing that rapamycin directly activates the cool-sensing ion channel, TRPM8, acting through a different binding site than other small-molecule cooling agents such as menthol. The use of Ca2+-imaging, electrophysiology, and computational biology provides **solid** evidence to support the finding. The authors also present a novel NMR-based method to help identify details of the binding site interactions. In this revised version, some analysis and the presentation have been corrected and improved. Their findings provide insights into TRP channel pharmacology and may indicate previously unknown physiological effects or therapeutic mechanisms of the immunosuppressant, rapamycin.

https://doi.org/10.7554/eLife.97341.2.sa4

Abstract

Rapamycin (sirolimus), a macrolide compound isolated from the bacterium *Streptomyces hygroscopicus*, is widely used as oral medication for the prevention of transplant rejection and the treatment of lymphangioleiomyomatosis. It is also incorporated in coronary stent coatings to prevent restenosis and in topical preparations for the treatment of skin disorders. Rapamycin's *in vivo* activities are generally ascribed to its binding to the protein FKBP12, leading to potent inhibition of the mechanistic target of rapamycin kinase (mTOR) by the FKBP12-rapamycin complex. The specific rapamycin-induced interaction between domains

from mTOR and FKBP12 is also frequently employed in cell biological research, for rapid chemically-induced protein dimerization strategies. Here we show that rapamycin activates TRPM8, a cation channel expressed in sensory nerve endings that serves as the primary cold sensor in mammals. Using a combination of electrophysiology, Saturation Transfer Triple-Difference (STTD) NMR spectroscopy and molecular docking-based targeted mutagenesis, we demonstrate that rapamycin directly binds to TRPM8. We identify a rapamycin-binding site in the groove between voltage sensor-like domain and the pore domain, distinct from the interaction sites of cooling agents and known TRPM8 agonists menthol and icilin. Related macrolide immunosuppressants act as partial TRPM8 agonists, competing with rapamycin for the same binding site. These findings identify a novel molecular target for rapamycin and provide new insights into the mechanisms of TRPM8 activation, which may assist in the development of therapies targeting this ion channel. Moreover, our findings also indicate that caution is needed when using molecular approaches based on rapamycin-induced dimerization to study ion channel regulation.

Introduction

TRPM8, a member of the Transient receptor potential (TRP) superfamily of cation channels, has been extensively studied in the context of sensory perception and thermoregulation (Iftinca & Altier, 2020; Kashio & Tominaga, 2022; Vriens et al., 2014). It is highly expressed in a subset of somatosensory neurons, where it acts as the principal molecular detector of decreases in temperature (Bautista et al., 2007; Colburn et al., 2007; Dhaka et al., 2007; McKemy et al., 2002; Peier et al., 2002). TRPM8-deficient mice have pronounced deficits in their response to cool and warm temperatures, do not exhibit cold-induced analgesia and also fail to detect mild warming of the skin (Bautista et al., 2007; Colburn et al., 2007; Dhaka et al., 2007; Paricio-Montesinos et al., 2020). In addition, TRPM8 expression is increased in various malignancies, making it a potential target or biomarker for cancer treatments (Ochoa et al., 2023).

Interestingly, TRPM8 is not only activated by cooling, but also by natural or synthetic cooling agents such as menthol or icilin (McKemy et al., 2002; Peier et al., 2002; Voets et al., 2004). Whereas the conformational changes that lead to cold-induced activation of TRPM8 remain largely elusive, the binding sites of menthol analogs and icilin have been resolved in high detail, based on site-directed mutagenesis studies and high-resolution cryo-EM structures (Bandell et al., 2006; Diver et al., 2019; Voets et al., 2007; Xu et al., 2020; Yin et al., 2019; Yin et al., 2018; Yin et al., 2022). These studies reveal that menthol binds in the cavity between the four alfa-helices of the voltage sensor-like domain (S1-S4), at a position halfway the membrane, where it interacts with residues in S2 and S4 (Xu et al., 2020; Yin et al., 2018). Icilin binds in the same cavity, but slightly closer to the cytosolic side of the membrane, in a binding mechanism that is potentiated by cytosolic calcium (Diver et al., 2019; Zhao et al., 2022). Furthermore, activity of TRPM8 is tightly regulated by the membrane lipid phosphatidylinositol-4,5-bisphosphate (PIP_2), which binds to an interfacial cavity formed by the outside surface of S4, S5 and several cytosolic domains (Diver et al., 2019; Rohacs et al., 2005; Yin et al., 2019).

Rapamycin is a chemical compound isolated from the bacterium *Streptomyces hygroscopicus*, which was first discovered in a soil sample on Easter Island (Rapa Nui) (Abraham & Wiederrecht, 1996). Initially described as an antifungal agent (Vezina et al., 1975), it was later found to possess potent immunosuppressive properties (Abraham & Wiederrecht, 1996). Subsequent research has uncovered its diverse therapeutic potential, ranging from its use in preventing organ transplant rejection and coronary stent restenosis, to the treatment of lymphangioleiomyomatosis, skin disorders, cancer and age-related diseases (Abraham & Wiederrecht, 1996; Ali et al., 2022; McCormack et al., 2011; Morice et al., 2002; Selvarani et al., 2021; Swarbrick et al., 2021). The various biological and therapeutic effects of rapamycin are primarily attributed to inhibition of mechanistic target of rapamycin kinase (mTOR). Rapamycin binds to the protein FKBP12,

leading to an inhibitory interaction of the FKBP12-rapamycin complex with the FRB (FKBP12-rapamycin binding) domain of mTOR (Abraham & Wiederrecht, 1996). The ability of rapamycin and rapamycin analogs to rapidly and efficiently bring FKBP12 and the FRB-domain in close contact has also been successfully engineered for the rapid chemical dimerization and translocation of signaling enzymes or receptors (Muthuswamy et al., 1999), including (TRP) ion channels (Suh et al., 2006; Varnai et al., 2006).

While performing experiments involving rapamycin-induced membrane translocation of a phospholipid phosphatase, we serendipitously discovered that rapamycin by itself potently activates TRPM8, both in TRPM8-expressing HEK cells and in mouse somatosensory neurons. Using whole-cell and inside-out patch-clamp recordings and Saturation Transfer Triple-Difference (STTD) NMR spectroscopy, we demonstrate that channel activation is caused by direct binding of rapamycin to TRPM8, rather than via an effect on mTOR activity. Based on site-directed mutagenesis guided by molecular docking, we provide evidence for a rapamycin-interaction site in the groove between S4 and S5, distinct from the known interaction sites for menthol or icilin. We also show that related macrolides such as the immunosuppressant everolimus act as partial TRPM8 agonists, and compete with rapamycin for the same binding site. Our results identify TRPM8 as a novel molecular target for rapamycin, and provide new insights into the mechanisms of TRPM8 activation, which may assist in the development of drugs targeting this ion channel. Finally, our results imply that direct activation of TRPM8 may need to be taken into account when using rapamycin-based dimerization approaches to study cellular processes *in vitro* and *in vivo*.

Results

Rapamycin activates TRPM8

When performing Fura-2-based intracellular Ca^{2+} concentration ($[Ca^{2+}]_i$) measurements in HEK293 cells stably expressing human TRPM8 channels (HEK-M8 cells), we observed that rapamycin (10 μM) caused a robust increase in $[Ca^{2+}]_i$, comparable in amplitude to the response evoked by the prototypical TRPM8 agonist menthol at a concentration of 50 μM (**Figure 1A**). Responses to both rapamycin and menthol were fully inhibited by the specific TRPM8 antagonist AMTB N-(3-aminopropyl)-2-[(3-methylphenyl) methoxy] -N-(2-thienylmethyl) benzamide hydrochloride; 2 μM) (Lashinger et al., 2008) (**Figure 1A**). The effect of rapamycin was concentration-dependent, with saturating responses at concentrations ≥10 μM and an EC_{50} value of 3.8 ± 2.0 μM (**Figure 1B**). Similar results were obtained using a 96-well plate-based assay, where we obtained an EC_{50} value of 6.0 ± 0.3 μM at room temperature, which shifted to of 10.1 ± 0.2 μM at 37 °C (**Figure S1**). Likewise, in whole-cell patch-clamp measurements on HEK-M8 cells at room temperature, rapamycin (10 μM) evoked robust TRPM8 currents, which rapidly returned to baseline upon washout of rapamycin and were fully inhibited by AMTB (2 μM; **Figure 1C**). Half-maximal activation of whole-cell currents at +120 mV was obtained at a rapamycin concentration of 4.5 ± 1.8 μM (**Figure 1D**). Importantly, menthol and rapamycin did not evoke any detectable calcium signal or current increase in non-transfected HEK293 cells (**Figure S2** and **Figure 3C**).

Next, we tested other TRP channels involved in chemo- and thermosensation (Bamps et al., 2021) for their sensitivity to rapamycin (**Figure S3**). We did not observe any sizeable current responses to 30 μM rapamycin in HEK293 cells expressing TRPA1, TRPV1 or TRPM3, whereas large currents were measured in response to their respective agonists allyl isothiocyanate (AITC; 373±173 pA/pF at +120 mV; N=5), capsaicin (1733±677 pA/pF at +120 mV; N=4) and pregnenolone sulfate (PS; 270±71 pA/pF at +120 mV; N=5), respectively.

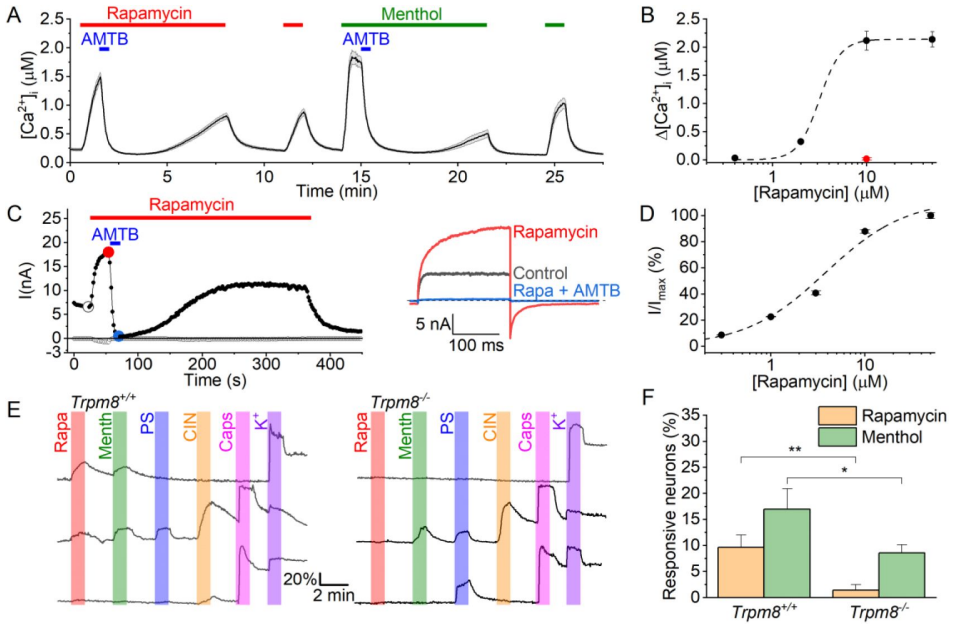

Figure 1

Rapamycin activates TRPM8 in HEK293 cells and sensory neurons.

(A) Time course of the intracellular calcium concentration in HEK293 cells expressing TRPM8, showing robust responses to rapamycin (10 μM) and menthol (50 μM), and inhibition of the responses by AMTB (2 μM). Shown are mean ± SEM, N=63 cells
(B) Concentration dependence of rapamycin-evoked calcium responses. The dashed line respresents the best fit using a Hill equation (EC_{50}=3.1; n_H=3.8). Shown are mean ± SEM, N=52-95 cells/concentration. The red symbol indicates the lack of response to rapamycin (10 μM) in non-transfected HEK293 cells (N=23).
(C) *Left,* time course of whole-cell currents in HEK293 cells expressing TRPM8 evoked by repetitive voltage steps to +120 and -80 mV, showing the activation of outwardly rectifying currents by rapamycin (10 μM) and inhibition by AMTB (2 μM). *Right,* voltage steps recorded at the indicated time points.
(D) Concentration dependence of rapamycin-evoked whole-cell currents at +120 mV. The dashed line respresents the best fit using a Hill equation (EC_{50}=3.8; n_H=1.0). Shown are mean ± SEM, N=5 cells per concentration
(E) Examples of calcium signals in individual DRG neurons from $Trpm8^{+/+}$ and $Trpm8^{-/-}$ mice in response to rapamycin (Rapa; 10 μM), menthol (Menth; 50 μM), pregnenolone sulphate (PS; 40 μM), cinnamaldehyde (CIN; 10 μM), capsaicin (Caps; 100 nM) or high K^+ (50 mM).
(F) Fraction of sensory neurons from $Trpm8^{+/+}$ and $Trpm8^{-/-}$ mice that responded to rapamycin and menthol.

TRPM8 is expressed in a small subpopulation (5-10%) of somatosensory neurons, where it plays a central role in detection of cool and warm temperature (Bautista et al., 2007; Colburn et al., 2007; Dhaka et al., 2007; McKemy et al., 2002; Paricio-Montesinos et al., 2020; Peier et al., 2002). To evaluate whether rapamycin activates TRPM8 in these neurons, we performed Fura-2-based calcium imaging experiments on somatosensory neurons isolated from the dorsal root and trigeminal ganglia (DRG and TG) of wild type (*Trpm8*$^{+/+}$) and *Trpm8*$^{-/-}$ mice (**Figure 1E**). In wild type neurons, approximately 10% of DRG and TG neurons showed a robust calcium response to rapamycin (10 μM). The large majority (95%) of these rapamycin-responsive neurons also responded to menthol (50 μM). Importantly, responses to rapamycin were largely eliminated in DRG and TG neurons from *Trpm8*$^{-/-}$ animals, indicating that TRPM8 mediates rapamycin responses in sensory neurons (**Figure 1E,F**).

Notably, a subset (~7%) of both *Trpm8*$^{+/+}$ and *Trpm8*$^{-/-}$neurons responded to menthol but not to rapamycin (**Figure 1F**). These findings are in line with earlier studies demonstrating that menthol acts as an agonist of not only TRPM8 but also TRPA1 (Karashima et al., 2007; Xiao et al., 2008). In agreement herewith, we found that 92 ± 7% of the rapamycin-insensitive menthol-responsive neurons were also activated by the TRPA1 agonist cinnamaldehyde. Moreover, in experiments using the TRPM8 antagonist AMTB, we found that 2 μM AMTB fully inhibited the calcium responses to menthol and rapamycin in rapamycin-responsive *Trpm8*$^{+/+}$ neurons, whereas menthol responses in rapamycin-insensitive neurons were not inhibited by AMTB (**Figure S2**). Taken together, these findings indicate that rapamycin selectively activates TRPM8-positive sensory neurons, whereas menthol is less selective, exciting both TRPM8-positive and TRPA1-positive neurons.

Taken together, these data show that rapamycin activates TRPM8 in a heterologous expression system and in sensory neurons, and indicate that rapamycin is a more selective tool than menthol to identify TRPM8-positive sensory neurons.

Rapamycin is an agonist ligand directly binding to TRPM8

We initially considered the possibility that the rapamycin-induced activation of TRPM8 in both HEK293 cells and sensory neurons could occur downstream of its effects on mTOR. However, the rapid onset and reversibility of rapamycin's effect on TRPM8 currents, and the observation that low micromolar concentrations of rapamycin were required to induce detectable current activation (compared to the nanomolar concentrations of rapamycin required for mTOR inhibition) (Abraham & Wiederrecht, 1996; Varnai et al., 2006) spoke against an mTOR-dependent effect. Notably, rapamycin also activated TRPM8 when applied to the cytoplasmic surface of excised inside-out patches (**Figure 2A**), indicating that it acts on TRPM8 in a membrane-delimited manner. Based on these observations we examined whether rapamycin could exert an agonistic action on TRPM8 via direct binding of the compound to the channel protein.

To test a direct molecular interaction between rapamycin and TRPM8, and to obtain insights into the parts of the rapamycin molecule involved in the interaction, we developed the Saturation Transfer Triple-Difference NMR (STTD-NMR) method. (**Figure 2B-E**). This new approach allowed us to obtain a clean ^{1}H-STTD NMR spectrum, eliminating interference from any non-specific interactions present in complex cellular systems. The basic principle of the classical, one-dimensional saturation transfer difference ^{1}H NMR (1D STD-NMR) is that resonances are saturated by selective irradiation, and this saturation spreads over the whole protein molecule and its bound ligands via spin diffusion (Meyer & Peters, 2003). The signal attenuation of ligand ^{1}H resonances upon binding is evident in the saturation transfer difference (STD) spectrum, which is obtained by subtraction of two spectra, one recorded with and the other without the saturation of protein resonances. We calculated the difference of STD spectra (double-difference STD, STDD) (Claasen et al., 2005), one recorded on a cellular sample with rapamycin added (sample 1, STD-1 in **Figure 2B,C**) and the other without rapamycin (sample 2, STD-2 in **Figure 2B,C**). The resulting

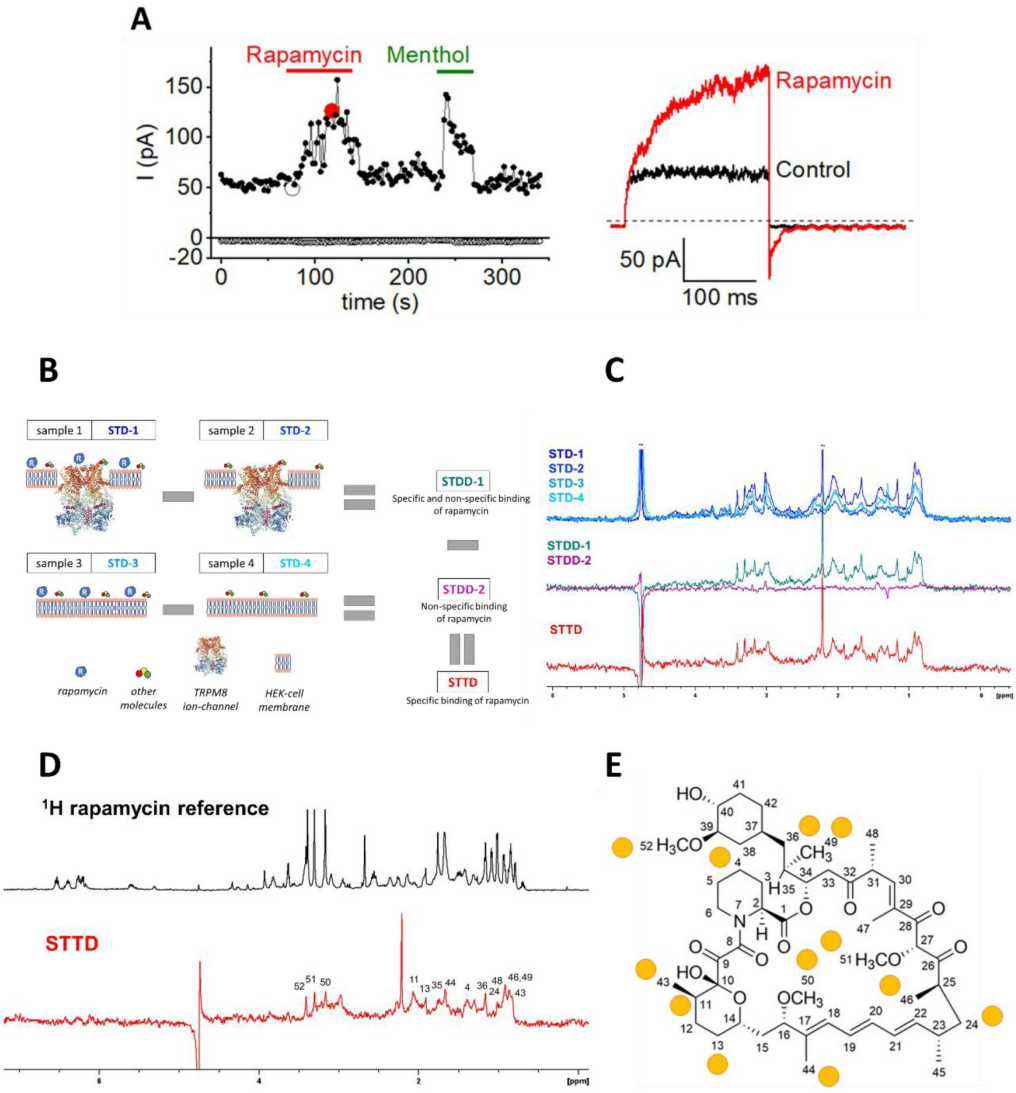

Figure 2

Direct interaction between rapamycin and TRPM8.

(A) *Left,* time course of currents in a cell-free inside-out patch pulled from a HEK293 cell expressing TRPM8 evoked by repetitive voltage steps to +80 and -80 mV, showing the activation of outwardly rectifying currents by rapamycin (10 μM) and menthol (50 μM) applied from the cytosolic side. *Right,* voltage steps recorded at the indicated time points. This example is representative for 5 similar experiments.
(B) Cartoon representing the steps to obtain the direct interaction of rapamycin with TRPM8. Individual STD spectra were recorded on different sample compositions, then non-specific interactions were filtered out with multiple subtractions resulting in the double difference spectra (STDD-1,2) and the final triple difference spectrum (STTD) shown on the right side.
(C) The four STD spectra (STD-1,2,3,4) are overlayed for comparison. Double difference spectra were computed from the respective STD pairs showing the specific and non-specific binding of rapamycin (STDD-1, green) and the non-specific binding of rapamycin alone (STDD-2, purple). All non-specific interactions were filtered out in the final STTD spectrum (red) computed by subtracting STDD-2 from STDD-1. Here, only one experimental set is shown (dataset B), spectra on the replicates can be found in the supplementary (Figures S5 and S6).
(D) Rapamycin resonances involved in the direct interaction with TRPM8 were assigned by the comparison of the reference ^{1}H NMR spectra of rapamycin (black) with the computed STDD effects (red). The reference spectrum was recorded on a 0.2 mM rapamycin sample in a D_2O buffer solution at 25 °C. The number of scans was 256 and a watergate sequence was used to suppress the residual water signal.
(E) Hydrogen atoms involved in the interaction with TRPM8 are mapped to the structure of rapamycin (yellow circles).

double-difference spectrum (STDD-1 in **Figure 2C**) reports both TRPM8 specific and non-specific binding interactions of rapamycin. To remove the STD signals arising from non-specific interactions of rapamycin, we recorded two more STD spectra on cells lacking TRPM8 expression (naïve HEK293 cells), namely in the presence (sample 3, STD-3) and absence (sample 4, STD-4) of rapamycin, yielding the second double-difference (STDD-2) spectrum (**Figure 2C**). Finally, the difference of STDD-1 and STDD-2 spectra yielded the triple-difference spectrum (STTD), which is free of interfering signals arising from any non-specific interactions (**Figure 2C**). To address the effect of the inherent variability of cellular samples on peak heights, STD effects were normalized based on the comparison of independent ^{1}H experiments (**Figure S5**). Three STTD replicates were computed, unambiguously confirming direct binding to TRPM8 in two datasets (**Figure S6A,B**). The signals assigned in the STTD spectra (numbered according to the schematic structure of rapamycin; **Figure 2D**) unveil the rapamycin H atoms that correspond to the binding epitopes of the molecule to TRPM8 (**Figure 2E**). Taken together, these findings indicate that rapamycin binds to TRPM8, acting as a direct channel agonist independently of mTOR.

In earlier work, we have classified TRPM8 agonists into two types based on their effect on the channel's gating kinetics (Janssens et al., 2016). According to this classification, Type I agonists such as menthol induce a slowing of the gating kinetics, which is most prominently observed as slowly deactivating tail currents following repolarization, whereas Type II agonists such as AITC cause an acceleration of the kinetics of channel activation upon depolarization, with little or no effect on the kinetics of deactivating tail currents. These differences in kinetics can be explained by a gating model where type I agonist cause a relative stabilization of the open state, whereas type II agonist rather destabilize the closed state (Janssens et al., 2016). Whole-cell current recordings in HEK-M8 cells revealed a pronounced effect of rapamycin on the kinetics of current relaxation in response to voltage steps (see e.g. **Figure 1C**; **Figure S7**). In particular, rapamycin caused a concentration-dependent slowing of the time course of voltage-dependent activation and deactivation, resulting in long-lasting tail currents upon repolarization from a strongly depolarizing voltage step to +120 mV, and these effects were more pronounced than for menthol (**Figure S7**). Overall, these characteristics classify rapamycin as a type I agonist, stabilizing the channel's open conformations. Notably, rapamycin and menthol had a synergistic effect on channel gating: application of menthol (50 μM) in the continued presence of rapamycin (10 μM) caused a further slowing down of channel deactivation (**Figure S8**).

Rapamycin binds to a unique binding site on TRPM8

Site-directed mutagenesis studies and high-resolution cryo-EM structures have delineated binding sites for several TRPM8 ligands, including agonists such as icilin, AITC, cryosim-3 and the menthol analog WS-12, as well as antagonists such as AMTB or TC-I 2014 (Bandell et al., 2006; Diver et al., 2019; Voets et al., 2007; Yin et al., 2019; Yin et al., 2018; Yin et al., 2022). These compounds all bind in the cavity between the four alfa-helices of the voltage sensor-like domain (S1-S4), with the exception of the type II agonist AITC, which binds outside the voltage sensor-like domain at a site between S3 and the S4-S5 linker (Yin et al., 2022).

Since rapamycin, like menthol, acts as a type I agonist, and both compounds contain a substituted cyclohexyl moiety, we initially examined the possibility that rapamycin would interact with the menthol-binding site. However, considering the much larger size of rapamycin (molecular weight of 914.2 g/mol) compared to agonists such as menthol, WS-12 or cryosim-3 (molecular weights of 154.3, 260.4 and 289.4 g/mol, respectively), binding of rapamycin in the relatively narrow cavity in the voltage sensor-like domain appeared unlikely. In agreement with this notion, initial experiments revealed that mutations in the menthol binding site that strongly reduce responses to menthol, icilin, Cooling Agent 10, WS-3 or cryosim-3 (Y745H and R842H) (Bandell et al., 2006; Voets et al., 2007; Malkia et al., 2009; Beccari et al., 2017; Plaza-Cayon et al., 2022; Yin et al., 2022; Palchevskyi et al., 2023) did not affect the channel's sensitivity to rapamycin (see **Figure 3**). Therefore, we hypothesized that rapamycin interacts at a different ligand binding site on TRPM8.

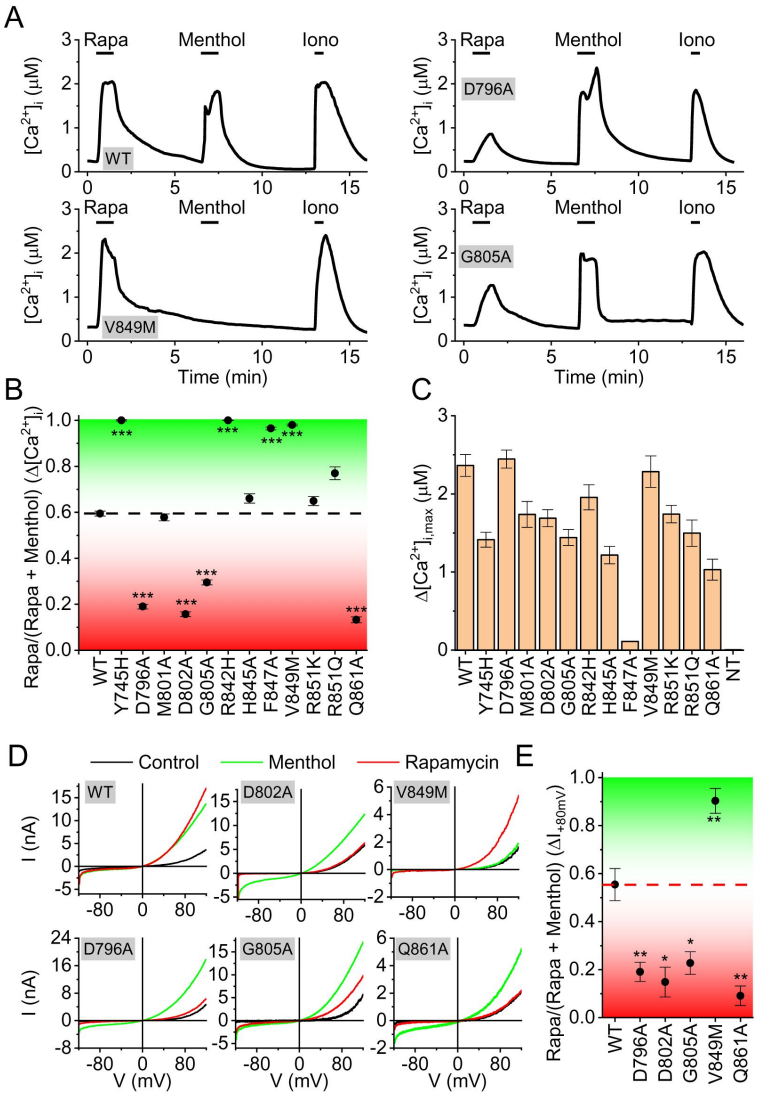

Figure 3

TRPM8 residues involved in the interaction with rapamycin and menthol.

(A) Representative time courses of the intracellular calcium concentration in HEK293 cells expressing wild type TRPM8 or the indicated mutants, when stimulated with rapamycin (10 μM), menthol (50 μM) and the calcium ionophore ionomycin (2 μM).
(B) Quantification of the relative calcium response to rapamycin and menthol for wild type and the indicated TRPM8 mutants. Values indicate the ratio between the calcium response amplitude to rapamycin, divided by the sum of the responses to rapamycin and menthol. The dotted line represents the mean value for wild type TRPM8. Values above this line (in yellow) indicate a relative reduction in the response to menthol, whereas values below the line (cyan) indicate a relative reduction in the response to rapamycin.
(C) Amplitude of the calcium response to the agonist (menthol or rapamycin) that gave the largest response for wild type and the indicated TRPM8 mutants. Data in B and C represent mean ± SEM, N=34-156/group.
(D) Whole-cell current-voltage relations for the currents in control, and in the presence of rapamycin (10 μM) or menthol (50 μM) in HEK293 cells expressing wild type TRPM8 or the indicated mutants. *, **, *** indicate p<0.05, p<0.01 and p<0.001 compared to WT.
(E) Quantification of the relative current response to rapamycin and menthol for wild type and the indicated TRPM8 mutants. Values indicate the ratio between the current amplitude increase at +80 mV to rapamycin, divided by the sum of the responses to rapamycin and menthol. The dotted line represents the mean value for wild type TRPM8. Values above this line (in yellow) indicate a relative reduction in the response to menthol, whereas values below the line (cyan) indicate a relative reduction in the response to rapamycin. Data in represent mean ± SEM; N=5-8 per mutant.

To identify potential rapamycin interaction sites, we performed blind, multistep dockings of rapamycin to a model of the human TRPM8 channel based on a cryo-EM structure of mouse TRPM8. Initial pilot dockings revealed several potential rapamycin interaction sites, either at the bottom of the voltage sensor-like domain or in the groove between the voltage sensor-like domain and the pore region (**Figure S9**). Based on these initial results, we made a series of point mutations at strategic residues in these potential rapamycin interaction sites, and used Fura-2-based $[Ca^{2+}]_i$ measurements to test these mutants for their responses to menthol (50 μM) and rapamycin (10 μM; **Figure 3A-C**). All mutant channels yielded robust calcium responses to at least one of the two agonists, indicating that they expressed as functional channels (**Figure 3C**). Wild type and most mutants showed maximal responses ($\Delta[Ca^{2+}]_i$) to at least one of the agonists of >1 μM. One exception was mutant F847A, which did not respond to menthol but showed a consistent but relatively small ($\Delta[Ca^{2+}]_i \asymp 200$ nM) to rapamycin (**Figure 3C** and **Figure S10**).

To assess potential changes in sensitivity to rapamycin or menthol, we calculated the rapamycin response ratio, defined as the calcium response to rapamycin over the sum of the calcium responses to rapamycin and menthol ($\Delta[Ca^{2+}]_{i,rapamycin}/(\Delta[Ca^{2+}]_{i,rapamycin} + \Delta[Ca^{2+}]_{i,menthol})$). As such, mutants that respond to rapamycin but fully lack a response to menthol have a response ratio of 1, while mutants that respond to menthol but fail to respond to rapamycin have a response ratio of 0. For the wild type channel, which robustly responds to both agonists, this analysis yielded a response ratio of 0.59 ± 0.02 (**Figure 3B**).

Several mutants yielded a significantly higher response ratio compared to wild type, indicating reduced menthol sensitivity. These included the previously described mutants Y745H and R842H (Bandell et al., 2006; Voets et al., 2007), which show robust responses to rapamycin but no responses to menthol (response ratios >0.95; **Figure 3A,B**). These residues, located in the middle of S1 and S4 respectively, point towards the center of the cavity within the voltage sensor-like domain, where they interact with ligands such as cryosim-3 and the menthol analog WS-12. Mutants R851Q and V849M, located at the cytosolic entrance to the cavity within the voltage sensor-like domain, also show a significantly reduced menthol response combined with a robust rapamycin response (response ratios of 0.77 ± 0.03, and 0.98 ± 0.02, respectively; **Figure 3A,B**). The results from these mutations are fully in line with the notion that menthol activates TRPM8 by binding in the middle of the cavity within the voltage sensor-like domain, and that mutations in the binding site or at the entrance of the cavity affect menthol activation. The observation that rapamycin activation is not noticeably affected in all these mutants confirms that the rapamycin and menthol binding sites are separate, and also argue against a potential rapamycin binding site at the lower part of the voltage sensor-like domain.

Oppositely, we identified four mutants with a significantly lower rapamycin response ratio compared to wild type (response ratios <0.3), indicating reduced rapamycin sensitivity. These include D796A (located in the S2-S3 linker), D802A and G805A (located in S3), and Q861A (located in the S5 pore helix; **Figure 3A,B**)). The strongly reduced sensitivity of these mutants to rapamycin was confirmed in whole-cell patch-clamp recordings, revealing robust current responses to menthol but very limited responses to rapamycin (**Figure 3D,E**). These results further confirm that rapamycin binds directly to the TRPM8 channel, and are in agreement with a model where rapamycin binds in the groove between the voltage sensor-like domain and the pore region. These results and the publication of the cryo-EM structure of the mouse TRPM8 during our experiments prompted the further refinement of dockings, resulting in the rapamycin binding site illustrated in **Figure 4** and **Figure S11** (the pdb-file of the model is available via *https://zenodo.org/records/14535771*). In this model, rapamycin interacts with residues from a single subunit. Note that this proposed mode of interaction also largely aligns with the results from the 1H-STTD NMR study, with several of the H atoms that show saturation transfer are effectively in close contact with the channel protein (**Figure S12**).

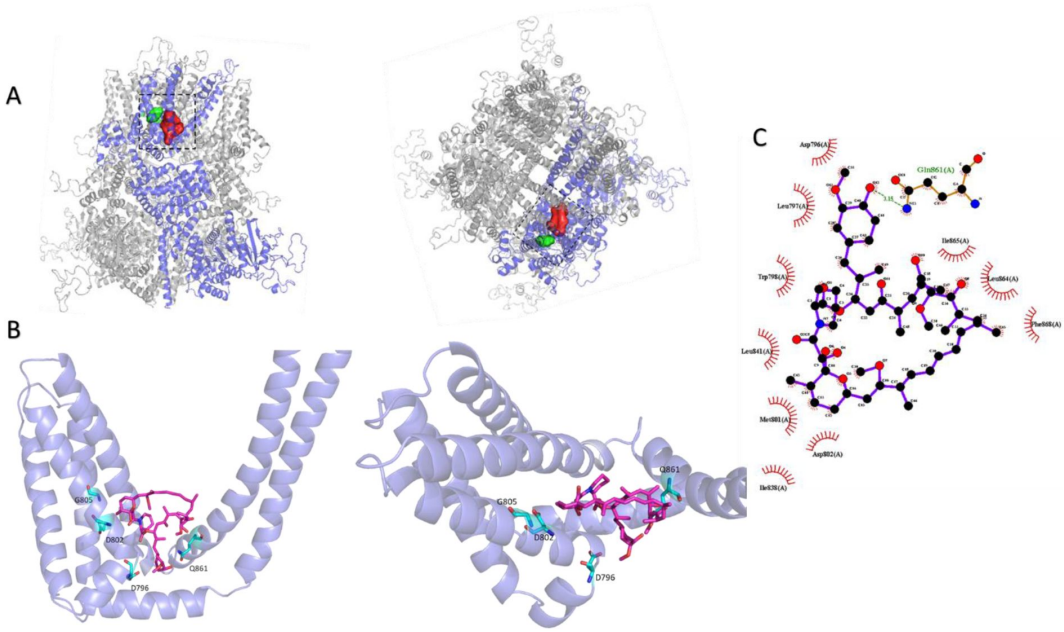

Figure 4

Structural model showing the distinct interaction sites for menthol and rapamycin.

(A) Side view (*left*) and top view (*right*) of TRPM8, showing the known interaction site for menthol (green) and the proposed rapamycin interaction site (red) based on our present molecular docking and mutagenesis studies.
(B) Closer view of rapamycin docked onto the TRPM8 structure. Amino acid residues that, when mutated, influence rapamycin responses are indicated in green.
(C) 2D projection of interactions between rapamycin and TRPM8 created using Ligplot^{+}.

Mutants D802A and G805A mutations were originally identified due to their ability to reduce icilin-induced activation of TRPM8 (Chuang et al., 2004). Interestingly, structural studies indicated that these residues are not directly involved in binding icilin. Instead, D802 is involved in calcium binding, which strongly potentiates activation of TRPM8 by icilin, while the flexibility invoked by a glycine at position 805 allows enlargement of the VSLD cavity to accommodate the hydroxyphenyl moiety of icilin (Yin et al., 2019). We therefore tested whether rapamycin activation is also modulated by intracellular calcium, by using UV flash-induced release of caged Ca^{2+} during whole-cell current recordings (Mahieu et al., 2010). In these experiments, a 1-ms UV flash was applied during a 800-ms voltage step to + 80 mV, either in the absence of ligand or in the presence of rapamycin (10 μM) or icilin (10 μM). The UV flash caused a rapid increase in intracellular Ca^{2+}, as indicated by the change in Fura-FF fluorescence ratio (**Figure 5A**). In line with our earlier work (Mahieu et al., 2010), at low cytosolic calcium icilin evokes a sizable current response, which is robustly potentiated of inward and outward currents in the presence of icilin (**Figure 5A-D**). In contrast, currents recorded in the absence of ligand or in the presence of rapamycin were not directly affected by flash-induced calcium uncaging (**Figure 5A-D**). These results demonstrate that rapamycin activation of TRPM8 is not calcium-dependent, and indicate that the reduced rapamycin sensitivity of the D802A mutant is unrelated to this residue's involvement in Ca^{2+} binding.

Effect of rapamycin analogs on TRPM8

According to the proposed binding mode (**Figure 4**), the substituted cyclohexane ring (*trans*-2-methoxycyclohexan-1-ol) of rapamycin is tightly involved in the interaction with TRPM8. In particular, the model predicts a hydrogen bond formed between Q861 and the hydroxyl group on the cyclohexane ring (i.e. on carbon 40 in the rapamycin structure). A number of rapamycin analogs (also known as rapalogs (Lamming et al., 2013)) have been developed as immunosuppressants, in which the hydroxyl group on the cyclohexane ring has been substituted by other functional groups. When tested using Fura-2-based calcium imaging, we found that everolimus, zotarolimus, ridaforolimus and temsirolimus were much less effective than rapamycin in activating TRPM8, with amplitudes that were <10% of that to rapamycin at a concentration of 10 μM (**Figure 6A,B**). The efficacy order was rapamycin >> zotarolimus > ridaforolimus > everolimus > temsirolimus. These results reveal the importance of the substituted cyclohexane ring, and in particular the hydroxyl group on carbon 40, for the activation of TRPM8 by rapamycin.

The calcineurin inhibitors FK506 (tacrolimus) and its structural analog ascomycin contain the same substituted cyclohexane ring (*trans*-2-methoxycyclohexan-1-ol)) as rapamycin, but have a different, smaller macrolactam ring than rapamycin and the rapalogs (**Figure 6A**). Confirming earlier research (Arcas et al., 2019), we found that FK506 evoked robust calcium responses in HEK-M8 cells, albeit less potently than rapamycin (**Figure 6B**). We also measured substantial responses to ascomycin, which were intermediate between were the responses to FK506 and to the most effective rapalog zotarolimus (**Figure 6B**). Pimecrolimus, a derivative of ascomycin in which a chloride substitutes for the corresponding hydroxyl group on the cyclohexane ring did not evoke any detectable calcium response (**Figure 6A,B**). Taken together, these findings demonstrate that rapamycin is the most effective of the tested macrolides, and illustrate the importance of the hydroxyl group at position 40 on the cyclohexane ring of rapamycin for activating TRPM8.

To investigate whether the substituted cyclohexane ring of rapamycin by itself is sufficient to evoke TRPM8 activation, we synthetized and tested *trans*-2-methoxycyclohexan-1-ol (2-metoxy-CHol). However, we could not detect any TRPM8 responses to 2-metoxy-CHol at concentrations up to 100 μM (**Figure 6A,B**), indicating that the 2-metoxy-CHol moiety is indispensable but insufficient for the activation of TRPM8.

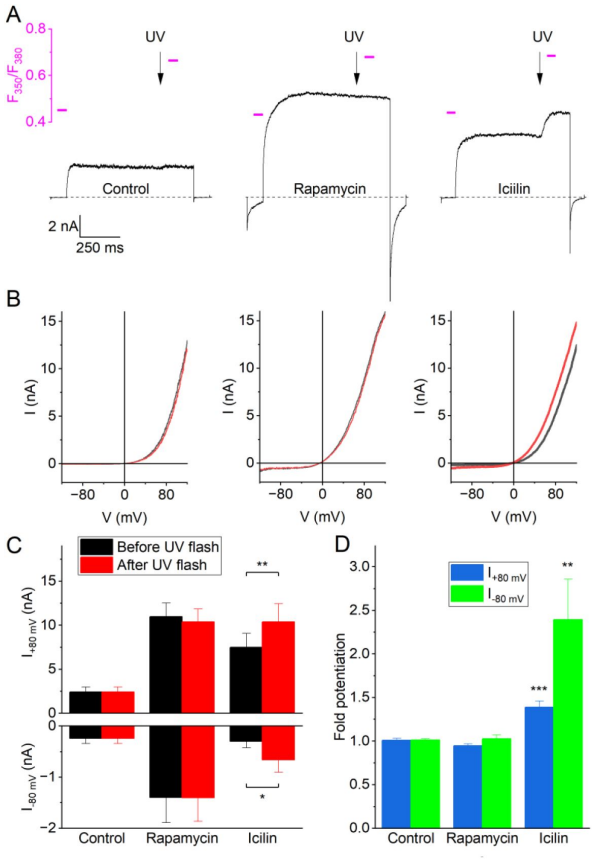

Figure 5

Activation of TRPM8 by rapamycin is independent of intracellular calcium.

(A) Whole-cell currents during 800-ms voltage steps from -80 to +80 mV under control conditions and in the presence of rapamycin (10 μM) or icilin (10 μM). At the time points indicated by the arrows, a 1-ms UV falsh was applied, leading to a rapid increase in intracellular calcium. Magenta lines and scale bar indicate Fura-FF fluoresence ratios at the indicated time points.
(B) Whole-cell current-voltage relations measured during voltage ramps 2 s before and 1 second after the UV flashes shown in panel A.
(C) Current amplitudes at +80 and -80 mV before and after UV uncaging of calcium, under control conditions and in the presence of rapamycin or icilin.
(D) Quantification of the relative potentiation of inward and outward currents following UV uncaging of calcium. Data in C and D represent the mean ± SEM from 5 experiments. *,**, ***: p<0.05 in a paired t-test comparing currents before and after UV flash.

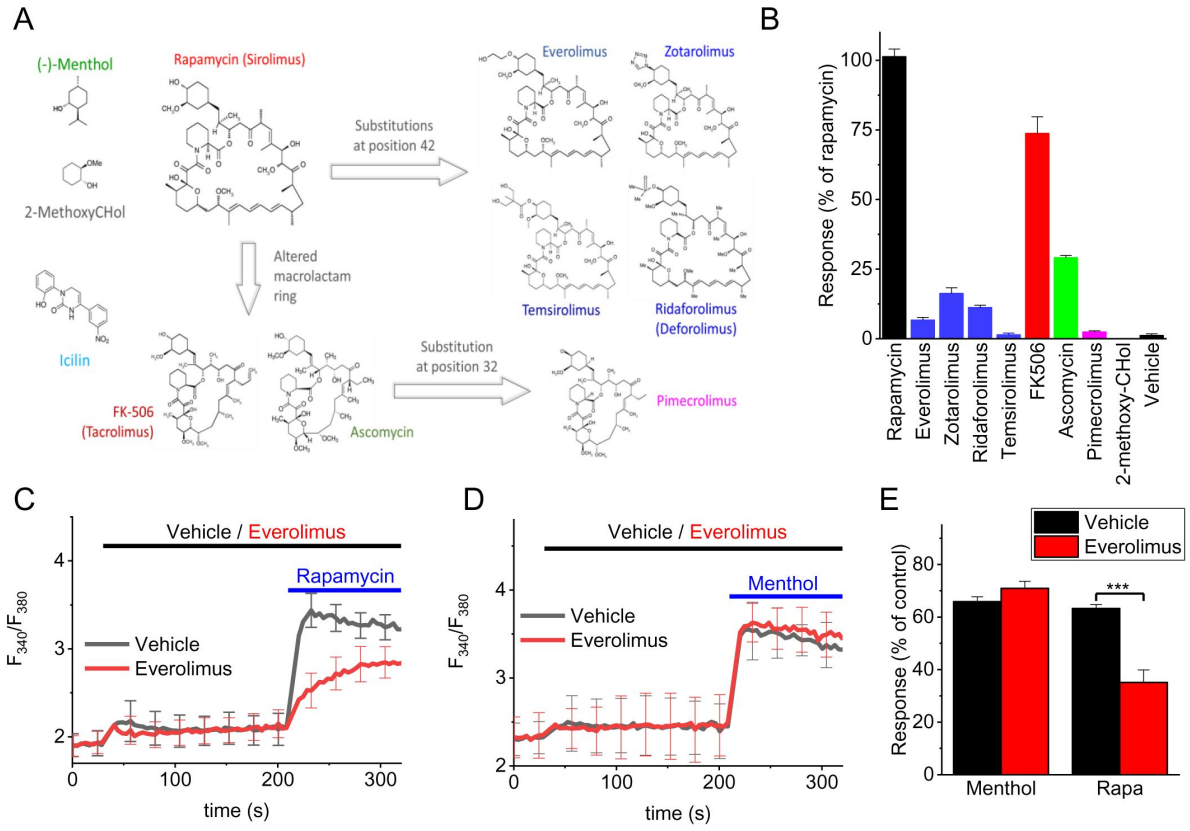

Figure 6

Effect of rapamycin and macrolid analogs on TRPM8.

(A) Overview of the macrolids tested in this study.
(B) Relative calcium response to rapamycin and the indicated analogs tested at 10 μM. N=6 in each group.
(C) Fura2-based calcium response to rapamycin (10 μM) in the presence of everolimus (10 μM) or vehicle. N=6 in each group.
(D) Fura2-based calcium response to menthol (50 μM) in the presence of everolimus (10 μM) or vehicle. N=6 in each group.
(E) Summary of the responses to menthol (50 μM) and rapamycin (10 μM) in the absence or presence of everolimus (10 μM). Responses were normalized to the response to a saturating concentration of menthol (300 μM). N=6 in each group. ***: p<0.001.

These findings raised the question whether the 2-metoxy-CHol moiety is essential for the binding of the macrolides to TRPM8, or rather affects the ability of the compounds to modulate the gating of TRPM8 following binding. To address this, we performed *in silico* dockings with everolimus, a close structural analog of rapamycin, in which the hydroxyl group on the cyclohexene ring is substituted by a 2-hydroxyethyl moiety. These revealed that everolimus can bind in the same region of TRPM8 as rapamycin, albeit with reduced binding energy (**Figure S13**). In particular, the docking indicated that substituting the hydroxyl group for the 2-hydroxyethyl moiety prevented the formation of a hydrogen bond with the amide of Q861 (**Figure S13**). If everolimus can indeed occupy the rapamycin binding site on TRPM8, without strongly activating the channel, the prediction would be that everolimus reduces the effect of rapamycin by competing for the same binding site. This was indeed confirmed in calcium imaging experiments showing that preincubation with 10 µM everolimus, a concentration which by itself does not evoke a substantial calcium signal, significantly inhibited the response to 10 µM rapamycin (**Figure 6C,E**). In contrast, 10 µM everolimus was without any effect on the response to 50 µM menthol (**Figure 6D,E**). Taken together, these findings indicate that macrolide analogs such as everolimus compete with rapamycin for the same binding site but with strongly reduced potency to activate the channel. The lack of effect on channel activation by menthol further confirms that the rapamycin and menthol binding sites are spatially separate and independent.

Discussion

Our study demonstrates that, in addition to its well-established inhibitory effect on the mTOR signaling pathway (Abraham & Wiederrecht, 1996; Lamming et al., 2013), rapamycin acts as an agonist of the ion channel TRPM8. Several lines of evidence indicate that the agonistic effect of rapamycin involves a direct interaction with the channel, rather than an indirect effect involving intracellular signaling pathways such as mTOR. First, we found that rapamycin rapidly and reversibly activates TRPM8 currents, not only in the whole-cell mode but also in inside-out patches, indicating a membrane-limited mode of action. Second, we developed STTD NMR methodology, which not only allowed us to demonstrate a direct molecular interaction between rapamycin and TRPM8, but also to identify moieties on rapamycin that interact with the channel. Finally, site-directed mutagenesis steered by molecular docking of rapamycin onto TRPM8 revealed residues that strongly reduce channel activation by rapamycin, while leaving responses to other stimuli intact. Although we cannot exclude that some of these mutations may have an allosteric effect on rapamycin-induced channel gating, the cumulative results are consistent with a model where rapamycin binds in the groove between the voltage sensor-like domain and the pore domain, at a site distinct from the interaction sites of well-studied TRPM8 agonists menthol and icilin.

The effect of rapamycin on TRPM8 occurs at low micromolar concentrations, which contrast to the low nanomolar concentrations required to inhibit mTOR signaling (Abraham & Wiederrecht, 1996; Varnai et al., 2006). Plasma concentrations of rapamycin in patients on systemic drug regimens following organ transplantation or for the treatment of lymphangioleiomyomatosis or cancer rarely exceed 100 nM (Jimeno et al., 2008; Trepanier et al., 1998), rendering it unlikely that substantial rapamycin-induced TRPM8 activation would occur in these subjects. However, rapamycin is also used topically for the treatment of skin diseases, with the use of creams or ointments containing millimolar concentrations of rapamycin. For instance, a 0.2% rapamycin gel (corresponding to approximately 2 mM) has been approved by the FDA for the treatment of facial angiofibromas in patients with tuberous sclerosis complex, and formulations up to 1% have shown efficacy in preclinical and clinical studies for this and other skin disorders, including psoriasis and oral lichen planus (Aitken et al., 2023; Ormerod et al., 2005; Soria et al., 2009). Following such treatments, local rapamycin concentrations are likely to rise to high-enough levels for activation of TRPM8 in sensory nerve endings of the skin, which could potentially contribute to beneficial effects of the drug in certain skin conditions. Indeed, it is well established that

activation of TRPM8 in sensory neurons has anti-inflammatory effects and causes relief of pain and itch (Liu et al., 2013; Palkar et al., 2018). Further research is required to elucidate the extent of this contribution and its clinical implications.

In addition to rapamycin, we also tested a comprehensive set of related macrolide immunosuppressants for their effect on TRPM8. In line with earlier work, FK506 also robustly activates TRPM8 (Arcas et al., 2019), albeit with lower potency than rapamycin, whereas the other tested macrolides had only very modest effects. Overall, these findings indicate that the *trans*-2-methoxycyclohexan-1-ol moiety is crucial for activity at TRPM8. Indeed, substitutions at this site (as for instance in everolimus) almost fully abolish TRPM8-mediated responses, whereas activity is at least partially maintained in compounds where this moiety is retained but with altered macrolactam ring (as in FK506 or ascomycin). These findings indicate that the structural determinants for macrolide activation of TRPM8 differ from the determinants for immunosuppressant activity, which are critically determined by the macrolactam ring (Chen & Zhou, 2020). Notably, we found that everolimus can inhibit activation of TRPM8 by rapamycin but not by menthol, indicating that it likely competes with rapamycin for the same binding site.

Overall, our data are consistent with a macrolide binding site on TRPM8, in the groove between voltage sensor-like domain and the pore domain, distinct from the interaction sites of cooling agents and known TRPM8 agonists menthol and icilin, but partially overlapping with the binding site of AITC. The existence of this binding site is also coherent with the finding of Acras et al. showing that TRPM8 sensitivity to FK506/tacrolimus is not affected by Y745H and N799A mutations which eradicate TRPM8 sensitivity to menthol and icilin, respectively. Notable, this groove is also involved in the binding of the antagonist NDNA in the closely related TRPM5 channel. Alignment of TRPM8 with other TRPM channels indicates that some of the key residues for rapamycin activation (D796 and D802) are conserved amongst other TRPM channels, whereas residue Q861 is unique for TRPM8 and G805 is only found in TRPM8 and TRPM2 (Huffer et al., 2020). Further studies may elucidate whether introduction of these residues may transfer rapamycin sensitivity to other TRPM channels. Moreover, structural alignment indicates that the rapamycin binding site in TRPM8 is in a similar location as the vanilloid binding site in TRPV1, although sequence alignment reveals that the key residues involved in binding are not conserved between these more distally related channels (Cao et al., 2013; Huffer et al., 2020; Kwon et al., 2021) The rapamycin binding site may provide a potential clue for the development of drugs that can selectively target TRPM8 for therapeutic purposes, without the side effects associated with other TRPM8 agonists. We acknowledge the limitations of our docking approach, which did not include the lipid bilayer and its interactions with the channel and ligand (Hughes et al., 2019). Nevertheless, the integration of docking with experimental validation, such as NMR and detailed calcium imaging and electrophysiology on selected mutants, strengthens the validity of our model. Interestingly, rapamycin also directly activates TRPML1, although information on a possible interaction site on that distally related channel are currently lacking (Zhang et al, 2019). We note that none of the key residues involved in activation of TRPM8 by rapamycin are conserved in TRPML1. Moreover, the order of potency of rapamycin analogs differs substantially between TRPML1 and TRPM8. For instance, TRPML1 is potently activated by temsirolimus, whereas this compound is without agonistic effect at TRPM8 (Zhang et al, 2019).

Finally, our results also serve as a cautionary note for the use of rapamycin in chemical dimerization studies, a common approach in the study of ion channels (Suh et al., 2006; Varnai et al., 2006). To exclude a contribution of TRPM8 in such experiments, the use of rapalogs such as everolimus represents a likely safer alternative.

In conclusion, our study reveals a hitherto undiscovered pharmacological property of rapamycin, identifying it as a direct agonist of the TRPM8 ion channel. These findings provide new insights into ligand activation of TRPM8, and may have potential therapeutic implications in the topical use of rapamycin for the treatment of skin diseases.

Methods

Cell culture and isolation of sensory neurons

Naive HEK293T cells and HEK293T cells stably overexpressing the human TRPM8 (HEK-M8 cells) were cultured at 37°C in DMEM medium supplemented with 10% fetal bovine serum, , 50 U/ml penicillin, 50 µg/ml streptomycin, 10 mM Glutamax, Non-Essential-Amino-Acids (all from Invitrogen/Thermo Fisher). G418 (500 µg/ml) was added to the medium of HEK-M8 cells.

Experiments using mice were approved by the KU Leuven Ethical Committee Laboratory Animals under project number P006/2014. All experimental procedures and animal husbandry were conducted following the European Parliament and the Council Directive (2010/63/EU) and national legislation. Sensory neurons of from the dorsal root and trigeminal ganglia (DRGs and TGs) were isolated from 8-16-week old wild type (*Trpm8*$^{+/+}$) and TRPM8-deficient (*Trpm8*$^{-/-}$) C57BL6 mice, as described before (Vandewauw et al., 2018). Briefly, mice were euthanized by CO_2, DRGs or TGs were isolated and digested with 1 mg/ml collagenase and 2.5 mg/ml dispase dissolved in 'basal medium' (Neurobasal A medium supplemented with 10% FCS) (all from Gibco/Thermo Fisher) at 37°C for ca. 45–60 min. Digested ganglia were gently washed once in 'basal medium' and twice in 'complete medium' (Neurobasal A medium supplemented with 2% B27 [Invitrogen/Thermo Fisher], 2 ng/ml GDNF [Invitrogen/Thermo Fisher] and 10 ng/ml NT4 [PeproTech, London, UK]) and mechanically dissociated by mixing with syringes fitted with increasing needle gauges. The suspension of sensory neurons was seeded on poly-L-ornithine/laminin-coated glass bottom chambers (Fluorodish, World Precision Instruments, Sarasota, FL USA) and maintained at 37°C for 24 to 36 hrs before experiments.

Microfluorimetric intracellular Ca^{2+} imaging

Fluorescent measurement of the cytoplasmic Ca^{2+} concentration in HEK cells and in individual sensory neurons were performed using the fluorescent Ca^{2+}-sensitive dye Fura-2 AM in various configurations, as reported earlier (Kelemen et al., 2021; Vandewauw et al., 2018).

To measure cytoplasmic Ca^{2+} concentration in individual neurons or HEK-M8 cells, a fluorescence microscope-based calcium imaging system was used. Cells were seeded in glass bottom chambers and next day, they were loaded with 2 µM Fura-2-AM (Invitrogen/Thermo Fisher Scientific) dissolved in normal Ca^{2+}-buffer (150 mM NaCl, 5 mM KCl, 1 mM $MgCl_2x6H_2O$, 2 mM $CaCl_2x2H_2O$, 10 mM glucose xH_2O, 10 mM HEPES, pH 7.4). Fura-2 signals were continuously captured (1 frame/s) using either a CellM (Olympus, Tokyo, Japan) or an Eclipse Ti (Nikon, Tokyo, Japan) fluorescence microscopy system. The cytoplasmic Ca^{2+} concentration was assessed by the ratio of fluorescence measured at λ_{EX1}: 340 nm, λ_{EX2}: 380 nm and λ_{EM}: 520 nm (F_{340}/F_{380}). During the measurements, cells were continuously perfused with buffer and different compounds were applied via rapid perfusion. Experiments were performed at room temperature.

To generate dose response curves and investigate rapalogs and other macrolides, we used a fluorescent microplate reader and monitored a population of HEK-M8 cells in each well. HEK-M8 cells were seeded in Poly-L-Lysine HBr coated 96-well black wall/clear-bottom plates (Greiner Bio-One, Frickenhausen, Germany) at a density of 100,000 cells per well in normal cell culture medium and incubated overnight. Next day, cells were loaded with 2 µM Fura-2-AM at 37°C for 30 min, and washed three times with Ca^{2+}-buffer. Then, changes in cytoplasmic Ca^{2+} concentration (indicated by the ratio of fluorescence measured at λ_{EX1}: 340 nm, λ_{EX2}: 380 nm, λ_{EM}: 510 nm (F_{340}/F_{380})) were measured using either a FlexStation 3 fluorescent microplate reader (Molecular Devices, Sunnyvale, CA, USA) or an FDSS/µCell analysis system (Hamamatsu Kinetic Plate Imager C13299). In some experiments. fluorescence signals were normalized to baseline values (F_0), and results

were expressed as $\Delta F/F_0$ to reflect the relative calcium dynamics. During the measurements, the tested compounds were applied in various concentrations using the built-in pipetting robot of the equipment. In each well, only one given concentration of the agents tested was applied. These measurements were carried out at ambient temperature or at 37 °C.

Patch clamp electrophysiology

HEK-M8 cells were seeded on poly-L-lysin coated glass coverslips and transmembrane currents were recorded in the whole-cell or inside-out configurations of the patch-clamp technique using a HEKA EPC-10 amplifier and Patchmaster software (HEKA Elektronik, Lambrecht/Pfalz, Germany). Data were sampled at 5-20 kHz and digitally filtered off-line at 1-5 kHz. Pipettes with final resistances of 2–5 MΩ were fabricated and used to establish a giga-seal access to the membrane. Unless mentioned otherwise, the holding potential was 0 mV and the following voltage step protocol was applied at 0.5 Hz: -80 mV for 200 ms, +120 mV for 200 ms, and -80 mV for 200 ms. In the whole-cell mode, between 70 and 90% of the series resistance was compensated. Whole-cell recordings were performed using an intracellular solution in the patch pipette containing (in mM) 150 NaCl, 5 MgCl2, 5 EGTA and 10 HEPES, pH 7.4 with NaOH. The extracellular solution contained (in mM) 150 NaCl, 1 MgCl2 and 10 HEPES, pH 7.4 with NaOH. In inside-out recordings, the extracellular solution was used as pipette solution, and ligands were applied via the intracellular bath solution.

In patch-clamp experiments where intracellular Ca^{2+} was manipulated through flash photolysis of caged Ca^{2+}, the pipette solution contained (in mM): 120 NaCl, 2 Fura-2FF and 20 HEPES, pH 7.4 with NaOH. This solution was further supplemented with 2 mM of the photolysable calcium chelator DM-nitrophen and 1.5 mM $CaCl_2$. Intracellular Ca^{2+} was monitored using a mono-chromator based system consisting of a Polychrome IV monochromator and photodiode detector (TILLPhotonics, Gräfelfing, Germany), controlled by Patchmaster software. Fluorescence was measured during excitation at alternating wavelengths (350 and 380 nm), corrected by subtraction of the back-ground fluorescence before establishing the whole-cell configuration, and represented as F_{350}/F_{380}. Rapid photolytic release of Ca^{2+} was achieved by subjecting the cell to brief (~1 ms) UV flashes applied from a JML-C2 flash lamp system (Rapp OptoElectronic GmbH, Hamburg, Germany), leading to step-wise, spatially uniform increases in intracellular Ca^{2+} (Mahieu et al., 2010).

Saturation Transfer Triple-Difference (STTD) NMR spectroscopy

^{1}H STD NMR experiments were performed on a Bruker Avance Neo 700 MHz spectrometer equipped with a 5-mm z-gradient Prodigy TCI cryoprobe. The temperature was maintained at 298 K. The ^{1}H reference experiments were run with 256 number of scans, a 1.2 s relaxation delay, and a watergate sequence was utilized for water suppression. These spectra were used to assess sample stability and to scale STD effects (**Figure S5**). A train of 50-ms Eburp1 (with B_1 field strength of 75 Hz) was employed for selective irradiation of protein ^{1}H resonances in total of 3 s. The saturation of aliphatic and aromatic proton regions of TRPM8 was carried out in separate experiments by setting the irradiation (on-resonance) frequencies of -1.8 ppm and 8.8 ppm, respectively, at least 2 ppm away from the resonances of rapamycin to avoid any partial saturation of rapamycin ^{1}H resonances. Reference spectra were recorded by setting the irradiation frequency off-resonance at -40 ppm. A spin-lock filter of 20 ms was applied to reduce the broad signals of the receptor and cell components in the resulting STD spectra. For each STD spectrum (the two on-resonance and one off-resonance) 640 number of scans was acquired in an interleaved fashion to average out any sample and/or spectrometer instability during the measurement, resulting in a total experiment time of 3 hours. All spectra were processed with Topspin version 4.0.5.

NMR samples: 25×10^6 HEK293T or HEK-M8 cells/sample were used. Cells were counted by a NovoCyte flow cytometer (Agilent Technologies), and the number of the functional TRPM8 channels were estimated as ca. 5000 channels/cell based on average whole cell currents and single

channels conductance available in the literature. 5 µl of rapamycin was added from a 22 mM stock solution resulting in a final concentration of 0.2 mM in D_2O PBS solution, providing ca. 4.8×10^7-fold excess of ligand to TRPM8 ion-channels for the STD NMR measurements. The final volume of each sample was 550 µl. NMR data was recorded in three replicates, a total of 12 individual samples were used to compute three independent STTD spectra (**Figure S6**).

Synthesis of trans-2-Methoxycyclohexan-1-ol

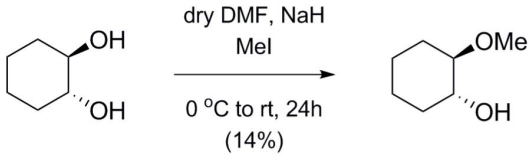

Trans-2-Methoxycyclohexan-1-ol was synthetized based on the method of Winstein and Henderson (Winstein & Henderson, 1943). To the solution of ***trans*-1,2-cyclohexanediol** (500 mg, 4.304 mmol) in dry DMF (19 mL) NaH (413 mg, 10.329 mmol, 60 m/m%, 1.2 equiv./OH) was added at 0°C. After 30 min stirring at that temperature 308 µl MeI (4.949 mmol, 1.15 equiv.) was added to the mixture and stirred for 24 h. When the TLC analysis (9:1 CH_2Cl_2/MeOH) showed complete consumption of the starting material, the reaction mixture was quenched by the addition of MeOH (2.5 mL). The solution was concentrated under reduced pressure and the residue was dissolved in CH_2Cl_2 (150 mL) washed with H_2O, dried on $MgSO_4$ and concentrated. The crude product was purified by column chromatography on silica gel (9:1 CH_2Cl_2/MeOH) to give ***trans*-2-methoxycyclohexan-1-ol** (80 mg, 14%) as a colorless syrup. $[\alpha]_D$ −6.54 (*c* 0.26, $CHCl_3$); R_f 0.47 (95:5 CH_2Cl_2/MeOH); ^{1}H NMR (400 MHz, $CDCl_3$) δ = 3.44-3.38 (m, 4H, OC*H*$_3$, H-1), 3.10 (s, 1H, H-1-O*H*), 2.94 (ddd, *J* = 10.6 Hz, *J* = 8.7 Hz, *J* = 4.4 Hz, 1H, H-2), 2.14-1.03 (m, 8H, 4 x C*H*$_2$), ppm; ^{13}C NMR (100 MHz, $CDCl_3$) δ = 85.0 (1C, C-2), 73.6 (1C, C-1), 56.3 (1C, O*C*H$_3$), 32.2, 28.4, 24.1, 24.0 (4C, 4x*C*H$_2$) ppm; MS (UHR ESI-QTOF): *m*/*z* calcd for $C_7H_{14}NaO_2$, $[M+Na]^+$ 153.0886; found: 153.0885.

Molecular docking

Initial docking simulations were performed using the cryo-EM structure of the full-length collared flycatcher (*Ficedula albicollis*) TRPM8 (pdb code: 6NR2, 83% sequence identity to human TRPM8) (Yin et al., 2019) high-resolution structures of rapamycin (pdb codes: 5FLC, 5GPG) retrieved from the RCSB Protein Data Bank.

Pilot dockings were performed using the Autodock 4.2 software in a 98.0 Å x 98.0 Å x 58.0 Å grid volume, large enough to cover the transmembrane domains of all four subunits of TRPM8 accessible from the extracellular side. The spacing of grid points was set to 1.0 Å and the whole target protein structure and the macrocyclic backbone of the ligand were kept rigid during dockings. 5000 dockings were performed with the above settings and the resultant rapamycin-TRPM8 complexes were clustered and ranked according to the corresponding binding free energies.

Internal flexibility of the rapamycin molecule was assessed through performing simulated annealing using the Gromacs 5.1.4 software package, the CHARMM36 force field and the GB/SA continuum solvent model. The simulated annealing protocol consisted of 2-ps gradual heating from 50 K to 1050 K, 5-ps equilibration at 1050 K and 5-ps exponential cooling back to 50 K. This protocol was repeated 1000 times for both crystallographic models of rapamycin. The coordinates of the system were stored after each simulated annealing cycle, resulting in a 1000-member ensemble of low-energy structures for both initial rapamycin models. Representative conformations of rapamycin were identified by clustering of the 1000-membered pools, having the macrocycle backbone atoms compared with 1.0 Å RMSD cut-off. Middle structures of the ten most populated clusters, accounting for more than 90% of the total conformational ensemble generated by simulated annealing, were used for further docking studies. To refine initial docking results

and to identify plausible binding sites, the above selected rapamycin structures were docked again to the protein target, following the same protocol as above, except for the grid spacing which was set to 0.375 Å in the second pass. The resultant rapamycin-TRPM8 complexes were, again, clustered and ranked according to the corresponding binding free energies. Selected binding poses were subjected to further refinement.

The three most populated and plausible binding poses were further refined by a third pass of docking, where amino acid side chains of TRPM8, identified in the previous pass to be in close contact with rapamycin (< 4 Å), were kept flexible. Grid volumes were reduced to these putative binding sites including all flexible amino acid side chains (21.0-26.2 Å x 26.2-31.5 Å x 24.8-29.2 Å). The spacing of grid points was maintained at 0.375 Å. Putative binding modes of rapamycin and TRPM8 were selected from the resultant low energy complexes on the basis of adherence to STTD-NMR data and the number of direct intermolecular contacts.

The initial dockings were further refined upon the publication of Cryo-EM structures of the mouse TRPM8 variant (Yin et al., 2022). The hTRPM8 protein sequence Q7Z2W7 was downloaded from the Universal Protein Resource (UniProt) and template Cryo-EM structures of mTRPM8 cold receptor in apo state C1 (PDB ID: 8E4N) and apo state C0 (PDB ID: 8E4P) were downloaded from the Protein Data Bank. The homology modelling was performed with the standard homology modelling protocol implemented in Yasara (*https://www.yasara.org*). Homology model based on these cryo-EM structures were performed using Swiss model as well with GMQE=0.71 and sequence identity=93.74%. All the structures were repaired using the FoldX plugin in YASARA, where RepairPDB identifies those residues which have bad torsion angles, or VanderWaals' clashes, or total energy, and repairs them. Visualization of the molecules was also done with Yasara. Figures were drawn with the open source Pymol (The PyMOL Molecular Graphics System, Version 2.5.2 Schrödinger, LLC; available at *https://www.pymol.org*). The global docking procedure was accomplished with Autodock VINA algorithms, implemented in Yasara, in which a total of 900 docking runs were set and clustered around the putative binding sites. The grid volumes and parameters were similar to those used for the third pass of docking, described above. The Yasara pH command was set to 7.0, to ensure that molecules preserved their pH dependency of bond orders and protonation patterns. The best binding energy complex in each cluster was stored, analyzed, and used to select the best orientation of the interacting partners. Using a similar docking strategy, we reproduced binding of menthol into the reported menthol binding site based on the cryo-EM structure of TRPM8 in complex with the menthol-analog WS-12 (Yin et al., 2019).

Generation of hTRPM8 mutants

Based on the results of the *in silico* studies, mutations were introduced at strategic sites within the putative ligand-binding domains. Single amino acids in the full length human TRPM8 sequence were mutated using the standard PCR overlap extension technique (Voets et al., 2007), and the nucleotide sequences of all mutants were verified by DNA sequencing. Constructs were cloned in the bicistronic pCAGGSM2-IRES-GFP vector, transiently expressed in HEK293 cells using TransIT-293 transfection reagent (Mirus, Madison, WI), and characterized using whole-cell patch-clamp electrophysiology and single cell calcium microfluorimetry as described above.

Chemicals

Rapamycin, FK506 ascomycin, everolimus, and temsirolimus were purchased from LC Laboratories (Woburn, MA USA). Unless indicated otherwise, all other chemicals were obtained from Sigma-Aldrich.

Data analysis and statistics

Data analysis and statistical tests were performed using Origin software (9.0 or 2023; OriginLab). Data are represented as mean ± SEM from *n* cells. One-way ANOVA with a Tukey post-hoc test was used to compare the effect of multiple mutations on TRPM8 ligand responses. Differences in the response profile of somatosensory neurons between genotypes were analyzed using Fisher's exact test. $P < 0.05$ was considered as statistically significant.

Concentration-response curves were fitted using the Hill equation of the form:

$$Response = \frac{Response_{max}}{1 + \left(\frac{EC_{50}}{[C]}\right)^{n_H}}$$

where the calculated parameters are the maximal calcium or current response ($Response_{max}$), the concentration for half-maximal activation (EC_{50}) and the Hill coefficient (n_H). To quantify ligand-induced changes in the time course of voltage-dependent current relaxation during voltage steps, mono-exponential functions were fitted to the current traces. While currents in the presence of agonists such as menthol or rapamycin become multiexponential, the monoexponential fits provide a robust quantification of changes in relaxation kinetics.

Supplementary figures

Figure S1

Rapamycin activates hTRPM8 in a concentration-dependent manner.

(A-B) Concentration dependence of rapamycin-evoked calcium responses measured by a microplate reader at room temperature (23 °C) (A) and 37°C (B). Shown are mean ± SEM; N=5 wells for each concentration. The lines represent the best fit using a Hill equation, yielding EC_{50} values of 6.0 ± 0.3 μM and 10.1 ± 0.2 μM, and Hill coefficients of 1.9 and 4.8, at 23°C and 37°C respectively.

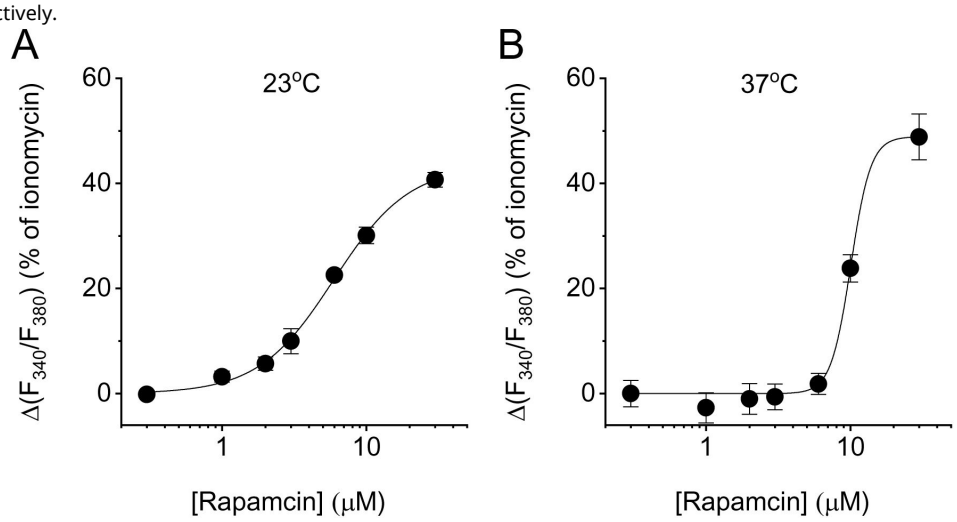

Figure S2

Rapamycin does evoke calcium signals in naïve HEK293 cells.

(A) Time course of the intracellular calcium concentration in non-transfected HEK293 cells, when stimulated with rapamycin (10 μM), menthol (50 μM) and the positive control stimulus ionomycin (2 μM). Shown are mean ± SEM, N=23 cells.
(B) Whole-cell current-voltage relations obtained in non-transfected HEK293 cells, using the same approach as used for wild type and mutant TRPM8 in **Figure 3D**. In N=5 similar experiments, changes in current amplitude upon addition of menthol or rapamycin never exceeded 50 pA at -100 and +100 mV.

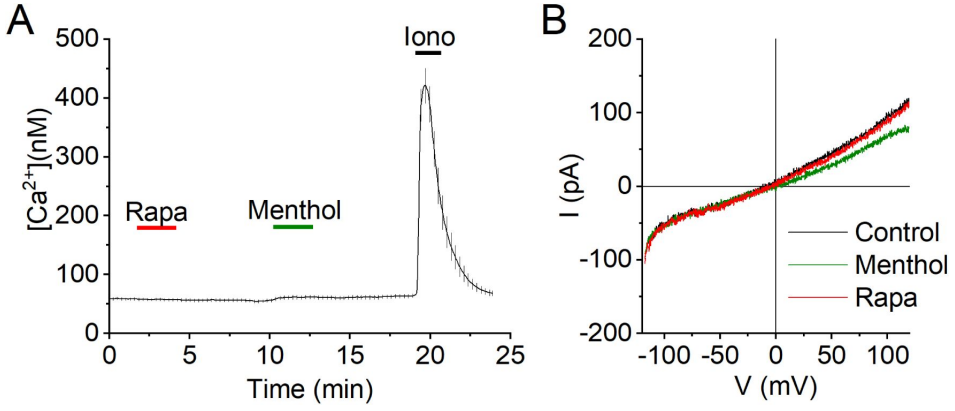

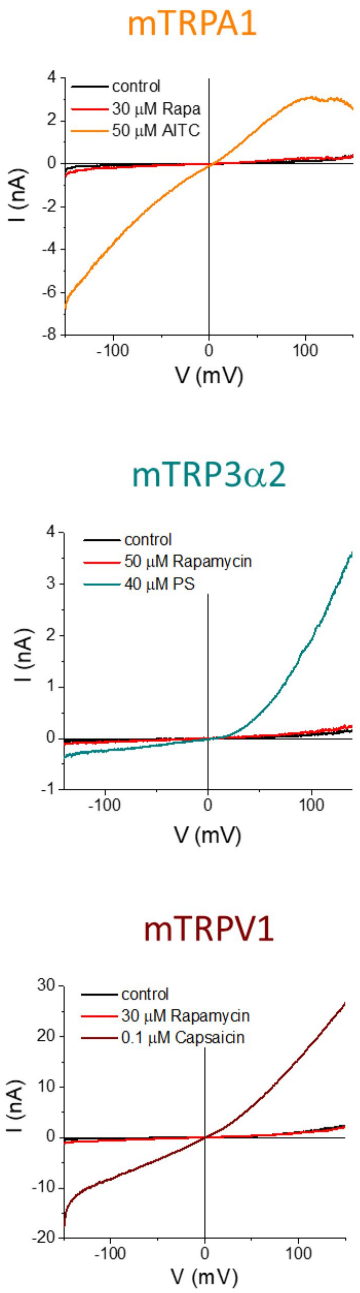

Figure S3

Rapamycin does not activate TRPA1, TRPM3 or TRPV1.

(A-C) Representative whole-cell current-voltage relations in CHO-cells expressing mouse TRPA1 (A), HEK293 cells expressing mouse TRPM3 (B) or HEK293 cells expressing human TRPV1 (C) upon stimulation with rapamycin (30 µM) or the respective agonists Allyl isothiocyanate (AITC), pregnenolone sulphate (PS; 40 µM) and capsaicin (Caps; 100 nM). Current responses to rapamycin where <5% of the response to the respective channel agonists in n=5 cells.

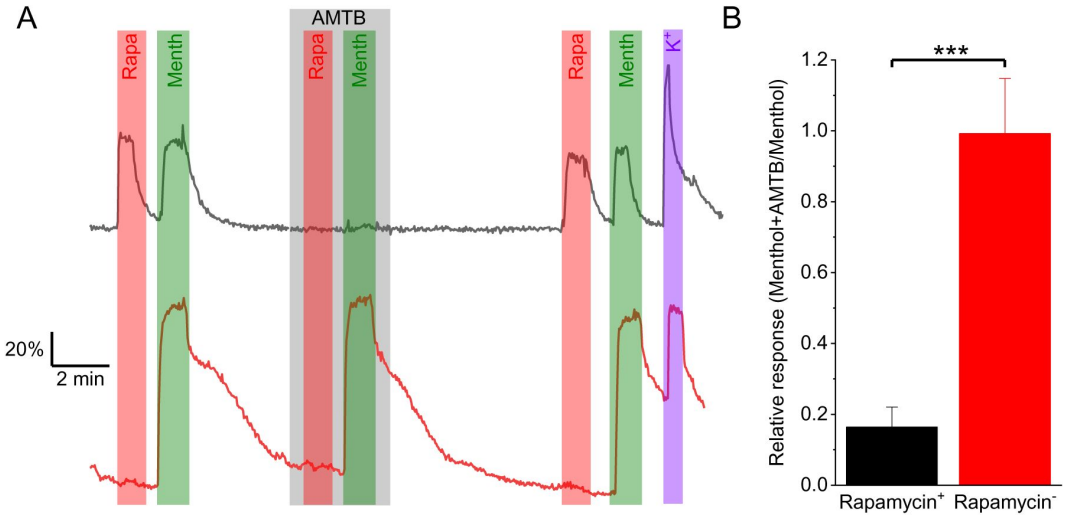

Figure S4

Rapamycin allows distinghuising between TRPM8-mediated and TRPM8-independent menthol responding sensory neurons.

(A) Representative examples of Fura2-based calcium signals in two sensory neurons that were stimulated three times at the indicated times with rapamycin (10 μM) or menthol (50 μM). During the second application, the TRPM8 antagonist AMTB was present at a concentration of 2μM.
(B) Average ratio between the response to menthol in the presence and absence of AMTB (second response/first response) in neurons that did or did not respond to rapamycin.

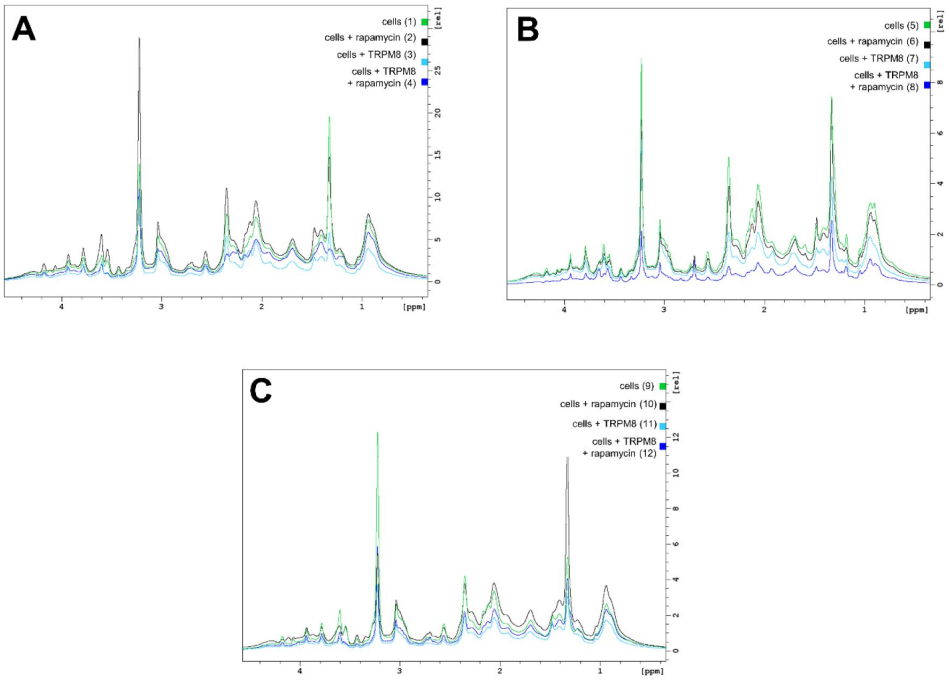

Figure S5.

The variability of peak heights in ^{1}H NMR experiments and the normalization procedure.

Reference ^{1}H experiments are shown on three individual sets of samples from which later three parallel STTD spectra were computed by the linear combinations of STD experiments. Conditions and sample numbering are shown in the right corner of the plots. The size of the spectra varied significantly despite the strict production protocol due to the complexity of the samples. Therefore, the scaling of the follow-up STD experiments was performed prior to the linear combinations based on the peak integral sums from the 0-4 ppm region of ^{1}H experiments. The corresponding STD spectra were scaled to an external spectrum recorded on a cell sample with an overexpressed ion channel and rapamycin. The following factors were used for multiplication: Dataset A: (1): 0.29, (2): 0.24, (3): 0.48, (4): 0.40. Dataset B: (5): 0.70, (6): 0.82, (7): 1.05, (8): 4.92. Dataset C: (9): 0.34, (10): 0.28, (11): 0.60, (12): 0.46.

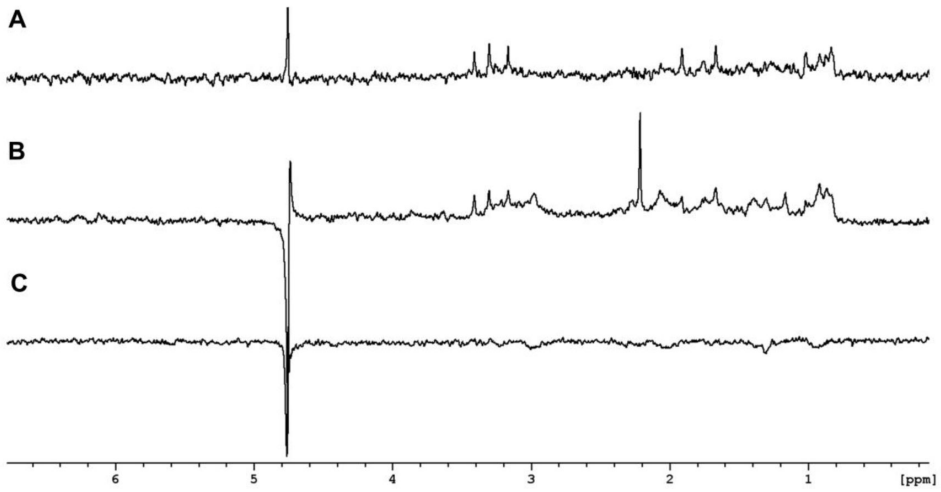

Figure S6.

Replicates of STTD measurements.

(A) An STTD spectrum obtained by the linear combinations of scaled STD spectra [(4-3) - (2-1)]. A direct interaction between rapamycin and the ion channel is confirmed and interaction sites of rapamycin were revealed upon peak assignments (presented in **Figure 2**).
(B) An STTD spectrum obtained by the linear combinations of scaled STD spectra [(8-7) - (6-5)]. A direct interaction between rapamycin and the ion channel is confirmed and the same interaction sites of rapamycin were revealed upon peak assignments.
(C) An STTD spectrum obtained by the linear combinations of scaled STD spectra [(12-11) - (10-9)]. Here, there is no reliable STD effect confirming the direct interaction between TRPM8 and rapamycin. Increased cell sedimentation was observed in sample 12 after measurements, an unconotrolled process that might have reduced the detected STD effects. Consequently the extent of non-specific binding outweighed specific binding resulting in zero or „negative" effects in the STTD spectrum.

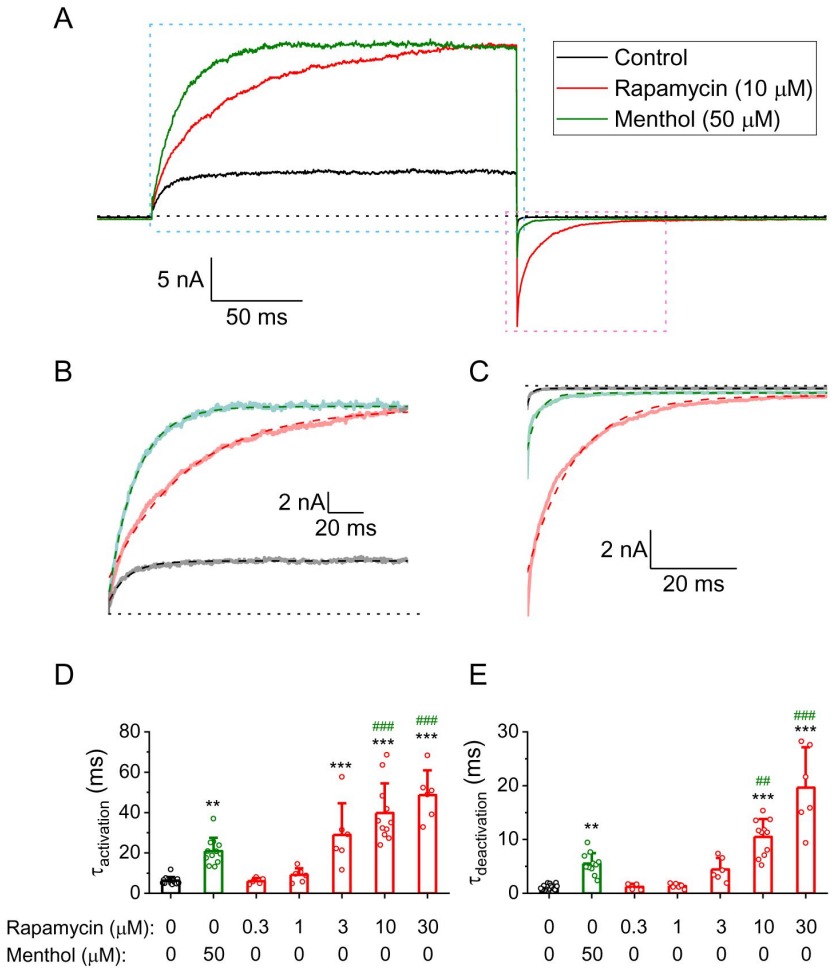

Figure S7

Rapamycin acts as a type I agonist.

(A) Representative examples of whole-cell currents in HEK293 cells expressing TRPM8, in response to a 200-ms voltage step from -80 to +120 mV and back to -80 mV, in control conditions and in the presence of the indicated concentrations of rapamycin or menthol.
(B) Zoomed-in time course of current relaxation at +120 mV. Dashed lines indicate monoexponential fits.
(C) Zoomed-in time course of current relaxation at -80 mV. Dashed lines indicate monoexponential fits.
(D) Monoexponential time constants for current activation at +120 mV in control conditions and in the presesence of the indicated concentrations of menthol or rapamycin.
(E) Monoexponential time constants for current deactivation at -80 mV in control conditions and in the presesence of the indicated concentrations of menthol or rapamycin. **, ***: P<0.01, P<0.001 *versus* control. $^{\#\#}$, $^{\#\#\#}$: P<0.01, P<0.001 *versus* menthol. Mean ± SD, dots represent individual cases.

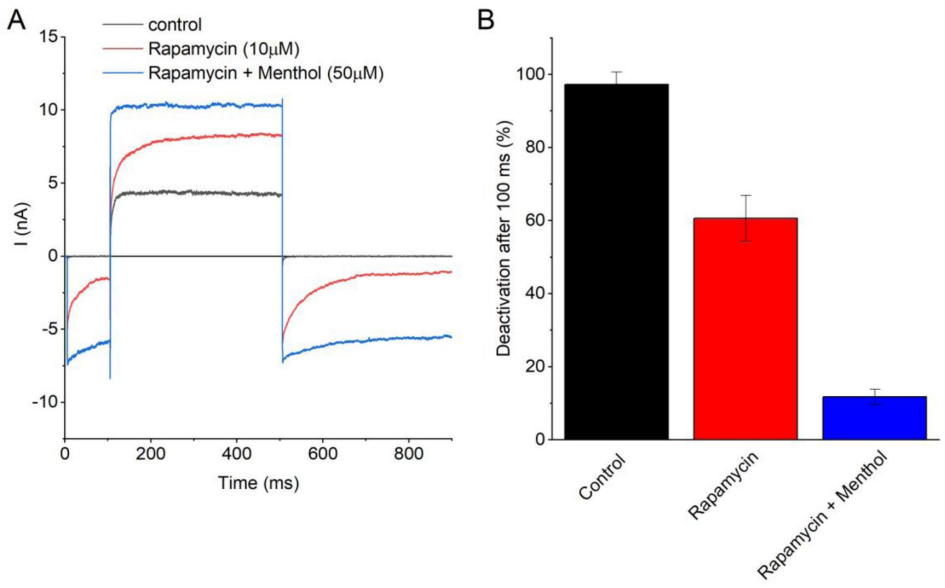

Figure S8

Additive effects of Rapamycin and menthol and TRPM8 deactivation.

(A) Representative examples of whole-cell currents in HEK293 cells expressing TRPM8, in response to a 200-ms voltage step from -120 to +120 mV and back to -120 mV, in control conditions, in the presence of rapamycin (10 μM) and in the combined presence of rapamycin (10 μM) and menthol (50 μM).
(B) Mean current deactivation, calculated as the fraction of the peak current upon the final step to -120 mV that deactivated after 100ms. Data from N=6 cells.

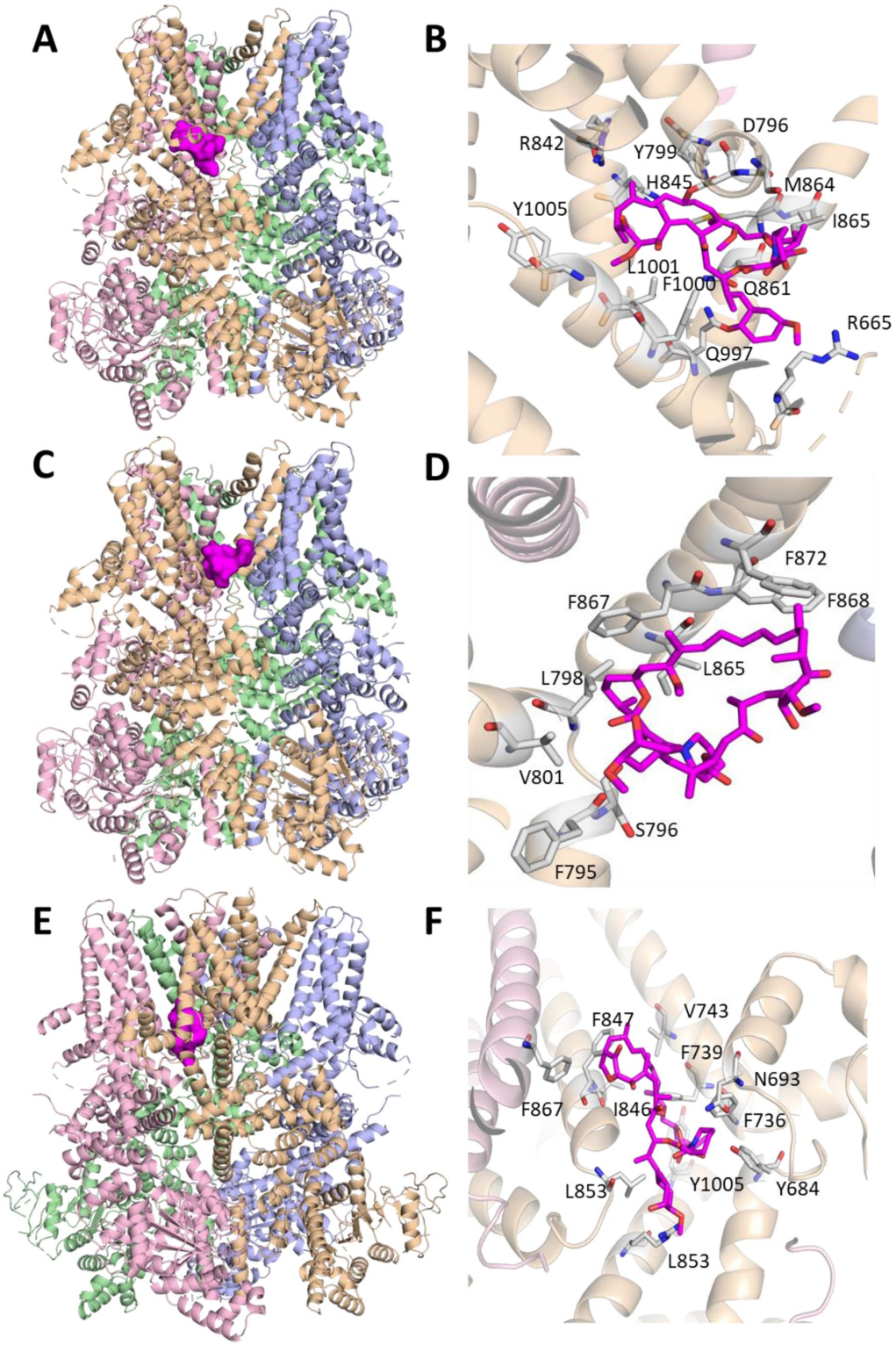

Figure S9.

Potential binding sites and poses of rapamycin on TRPM8 obtained from blind pilot dockings.

(A-B) site 1, (C-D) site 2, (E-F) site 3. Rapamycin was docked onto the structure of full-length TRPM8 from the collared flycatcher (*Ficedula albicollis*; pdb code: 6NR2). For clarity, the amino acid numbering refers to the corresponding residues in the human TRPM8 ortholog.

Figure S10

Rapamycin, but not menthol, moderately activates HEK cells expressing TRPM8^{F847A}

(A) Time course of the intracellular calcium concentration in HEK293 cells expressing TRPM8^{F847A}, showing moderate responses to rapamycin (10 µM) but no response to menthol (50 µM). Ionomycin was used as positive control. Shown are mean ± SEM, N=114 cells

(B) Statistical analysis on the amplitude of Ca^{2+} transients evoked by menthol (50 µM), rapamycin (10 µM) and ionomycin. Shown are mean ± SEM; N=114 cells.

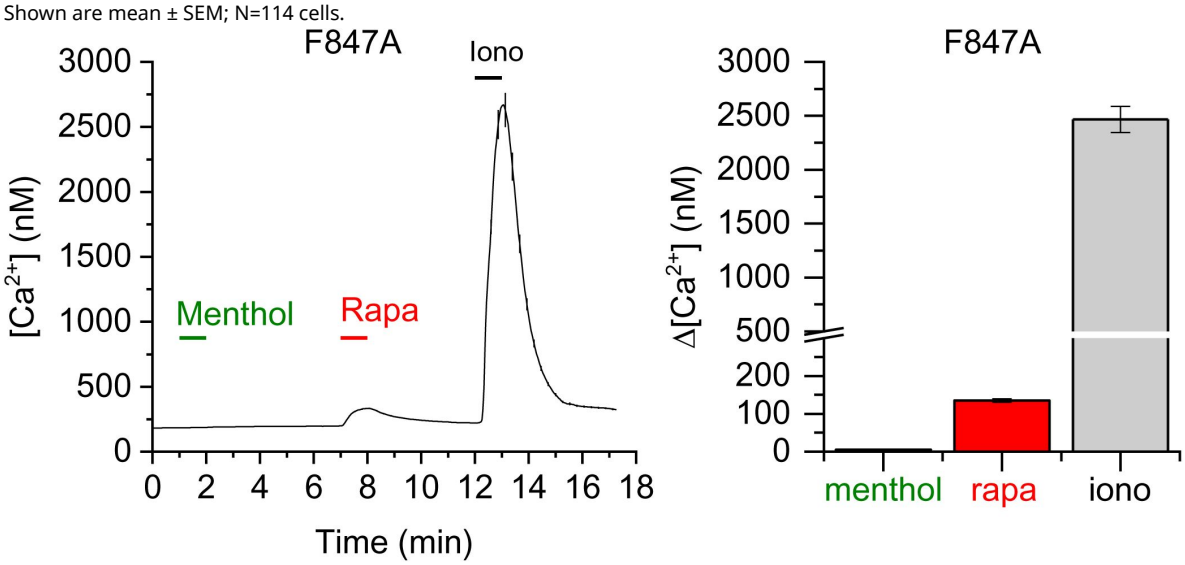

Figure S11

Structural model indicating side chains for all mutations, colored by menthol (green)/rapamycin (red) selectivity.

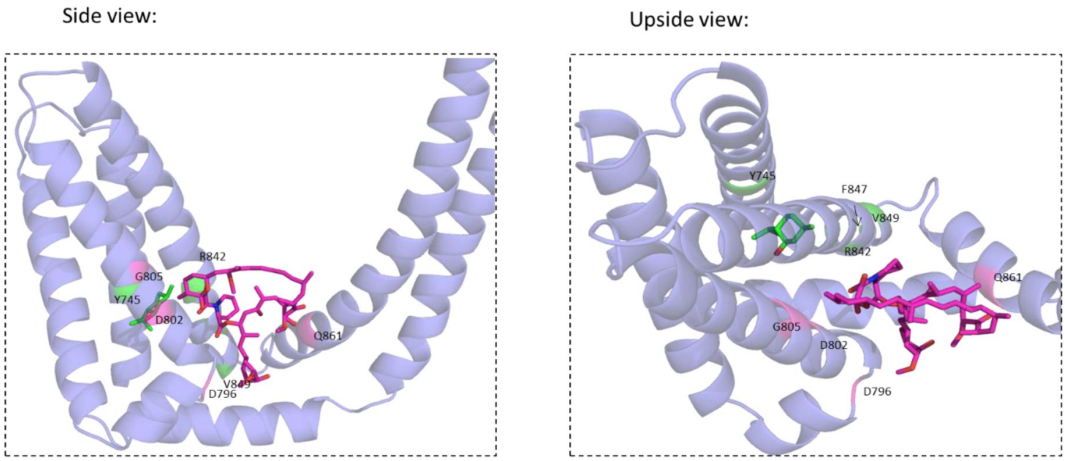

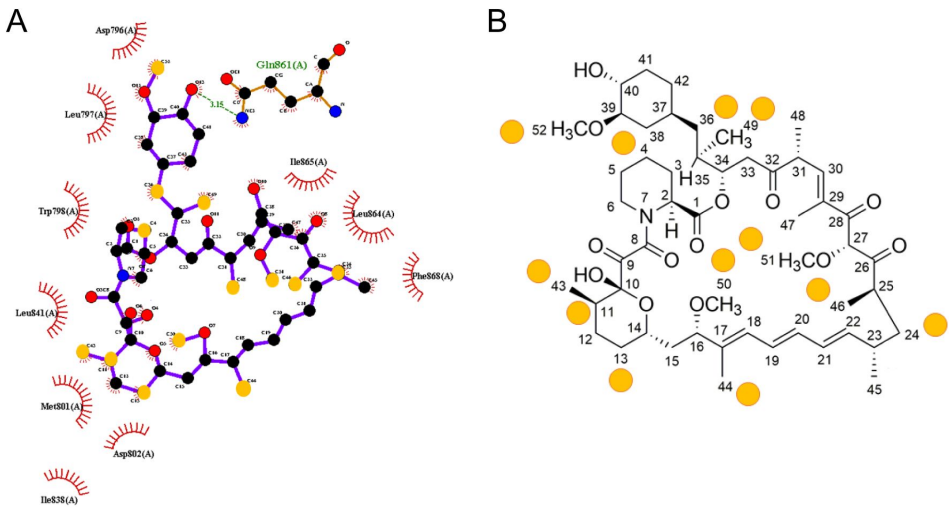

Figure S12

Visualizing and comparing the STTD NMR results with the predicted rapamycin binding pocket.

(A) 2D projection of interactions between rapamycin and TRPM8 created using Ligplot+. The yellow circles mark the carbon atoms of the rapamycin which the interacting hydrogen atoms identified by STTD NMR belong to.
(B) Structure of rapamycin indicating hydrogen atoms involved in the interaction with TRPM8. The interacting hydrogen atoms proposed by the STTD NMR experiments are marked by the yellow circles.

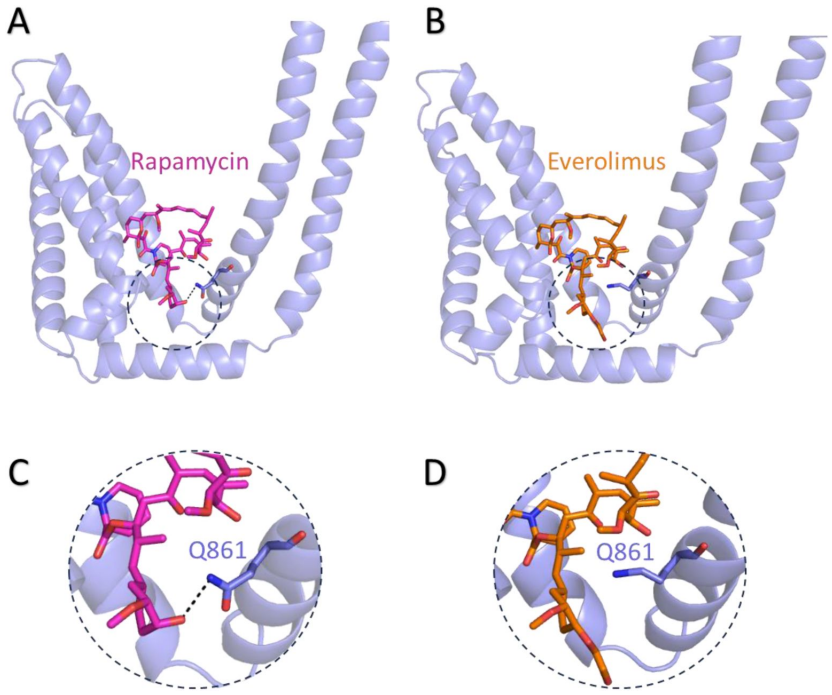

Figure S13.

Molecular docking of rapamycin and everolimus to the groove between voltage sensor-like domain and the pore domain of TRPM8.

(A-B) In silico molecular docking indicates that everolimus binds to TRPM8 in a similar pose as rapamycin, albeit with lower binding energy (-8.5 kcal/mol for everolimus versus -11.6 kcal/mol for rapamycin).
(C-D) A zoom-in on the binding site shows the hydrogen bond between the hydroxyl group on the cyclohexane ring in rapamycin (C) and the side-chain amide of residue Gln861, whereas no such a hydrogen bond can be formed between the longer hydroxyethyl moiety on everolimus (D).

Additional information

Funding statement

The presented work was supported by research grants of the National Research, Development and Innovation Office (grant numbers: 134725 for B.I.T., 134791 for E.L., 137924 for M.H. GINOP-2.3.2-15-2016-00050, GINOP-2.3.3-15-2016-00004, and GINOP-2.3.2–15-2016–00044). B.I.T. was awarded the János Bolyai Research Scholarship of the Hungarian Academy of Sciences. M.R., T.M.N. and B.I.T. were supported by the New National Excellence Program of the Ministry for Innovation and Technology [grant numbers ÚNKP-22-3-I-DE-324 and ÚNKP-23-3-II-DE-430 for M.R., UNKP-22-4-I-DE-87 for T.M.N., and ÚNKP-21-5-DE-491 for B.I.T.] Research in the lab of T.V. is supported by grants from the Research Foundation - Flanders (FWO; G0B9520N), the Research Council of KU Leuven (C2-TRP), the Queen Elisabeth Medical Foundation for Neurosciences and the VIB. The project has received funding from the EU's Horizon 2020 research and innovation program under grant agreement No. 739593.

References

Abraham R. T., Wiederrecht G. J 1996) **Immunopharmacology of rapamycin** *Annu Rev Immunol* **14**:483–510 https://doi.org/10.1146/annurev.immunol.14.1.483

Aitken P., Stanescu I., Boddington L., Mahon C., Fogarasi A., Liao Y. H., Ivars M., Moreno-Artero E., Trauner D., DeRoos S. T., Jancic J., Nikolic M., Balazova P., Price H. N., Hadzsiev K., Riney K., Stapleton S., Tollefson M. M., Bauer D., Atkinson H 2023) **A novel rapamycin cream formulation improves facial angiofibromas associated with tuberous sclerosis complex: a double-blind randomized placebo-controlled trial** *Br J Dermatol* **189**:520–530 https://doi.org/10.1093/bjd/ljad243

Ali E. S., Mitra K., Akter S., Ramproshad S., Mondal B., Khan I. N., Islam M. T., Sharifi-Rad J., Calina D., Cho W. C 2022) **Recent advances and limitations of mTOR inhibitors in the treatment of cancer** *Cancer Cell Int* **22**:284 https://doi.org/10.1186/s12935-022-02706-8

Arcas J. M., Gonzalez A., Gers-Barlag K., Gonzalez-Gonzalez O., Bech F., Demirkhanyan L., Zakharian E., Belmonte C., Gomis A., Viana F 2019) **The Immunosuppressant Macrolide Tacrolimus Activates Cold-Sensing TRPM8 Channels** *J Neurosci* **39**:949–969 https://doi.org/10.1523/JNEUROSCI.1726-18.2018

Bamps D., Vriens J., de Hoon J., Voets T. 2021) **TRP Channel Cooperation for Nociception: Therapeutic Opportunities** *Annu Rev Pharmacol Toxicol* **61**:655–677 https://doi.org/10.1146/annurev-pharmtox-010919-023238

Bandell M., Dubin A. E., Petrus M. J., Orth A., Mathur J., Hwang S. W., Patapoutian A 2006) **High-throughput random mutagenesis screen reveals TRPM8 residues specifically required for activation by menthol** *Nat Neurosci* **9**:493–500 https://doi.org/10.1038/nn1665

Bautista D. M., Siemens J., Glazer J. M., Tsuruda P. R., Basbaum A. I., Stucky C. L., Jordt S. E., Julius D 2007) **The menthol receptor TRPM8 is the principal detector of environmental cold** *Nature* **448**:204–208 https://doi.org/10.1038/nature05910

Beccari AR, Gemei M, Lo Monte M, Menegatti N, Fanton M, Pedretti A, Bovolenta S, Nucci C, Molteni A, Rossignoli A, Brandolini L, Taddei A, Za L, Liberati C, Vistoli G 2017) **Novel selective, potent naphthyl TRPM8 antagonists identified through a combined ligand- and structure-based virtual screening approach** *Sci Rep* **7**:10999 https://doi.org/10.1038/s41598-017-11194-0

Cao E., Liao M., Cheng Y., Julius D 2013) **TRPV1 structures in distinct conformations reveal activation mechanisms** *Nature* **504**:113–118 https://doi.org/10.1038/nature12823

Chen Y., Zhou X 2020) **Research progress of mTOR inhibitors** *Eur J Med Chem* **208**:112820 https://doi.org/10.1016/j.ejmech.2020.112820

Chuang H. H., Neuhausser W. M., Julius D 2004) **The super-cooling agent icilin reveals a mechanism of coincidence detection by a temperature-sensitive TRP channel** *Neuron* **43**:859–869 https://doi.org/10.1016/j.neuron.2004.08.038

Claasen B., Axmann M., Meinecke R., Meyer B 2005) **Direct observation of ligand binding to membrane proteins in living cells by a saturation transfer double difference (STDD) NMR spectroscopy method shows a significantly higher affinity of integrin alpha(IIb)beta3 in native platelets than in liposomes** *J Am Chem Soc* **127**:916–919 https://doi.org/10.1021/ja044434w

Colburn R. W., Lubin M. L., Stone D. J., Wang Y., Lawrence D., D'Andrea M. R., Brandt M. R., Liu Y., Flores C. M., Qin N 2007) **Attenuated cold sensitivity in TRPM8 null mice** *Neuron* **54**:379–386 https://doi.org/10.1016/j.neuron.2007.04.017

Dhaka A., Murray A. N., Mathur J., Earley T. J., Petrus M. J., Patapoutian A 2007) **TRPM8 is required for cold sensation in mice** *Neuron* **54**:371–378 https://doi.org/10.1016/j.neuron.2007.02.024

Diver M. M., Cheng Y., Julius D 2019) **Structural insights into TRPM8 inhibition and desensitization** *Science* **365**:1434–1440 https://doi.org/10.1126/science.aax6672

Huffer K. E., Aleksandrova A. A., Jara-Oseguera A., Forrest L. R., Swartz K.J. 2020) **Global alignment and assessment of TRP channel transmembrane domain structures to explore functional mechanisms** *eLife* **9** https://doi.org/10.7554/eLife.58660

Hughes T. E., Del Rosario J. S., Kapoor A., Yazici A. T., Yudin Y., Fluck E. C., Filizola M., Rohacs T., Moiseenkova-Bell V. Y 2019) **Structure-based characterization of novel TRPV5 inhibitors** *eLife* **8** https://doi.org/10.7554/eLife.49572

Iftinca M., Altier C 2020) **The cool things to know about TRPM8!** *Channels (Austin)* **14**:413–420 https://doi.org/10.1080/19336950.2020.1841419

Janssens A., Gees M., Toth B. I., Ghosh D., Mulier M., Vennekens R., Vriens J., Talavera K., Voets T 2016) **Definition of two agonist types at the mammalian cold-activated channel TRPM8** *eLife* **5** https://doi.org/10.7554/eLife.17240

Jimeno A., Rudek M. A., Kulesza P., Ma W. W., Wheelhouse J., Howard A., Khan Y., Zhao M., Jacene H., Messersmith W. A., Laheru D., Donehower R. C., Garrett-Mayer E., Baker S. D., Hidalgo M 2008) **Pharmacodynamic-guided modified continuous reassessment method-based, dose-finding study of rapamycin in adult patients with solid tumors** *J Clin Oncol* **26**:4172–4179 https://doi.org/10.1200/JCO.2008.16.2347

Karashima Y., Damann N., Prenen J., Talavera K., Segal A., Voets T., Nilius B 2007) **Bimodal action of menthol on the transient receptor potential channel TRPA1** *J Neurosci* **27**:9874–9884 https://doi.org/10.1523/JNEUROSCI.2221-07.2007

Kashio M., Tominaga M 2022) **TRP channels in thermosensation** *Curr Opin Neurobiol* **75**:102591 https://doi.org/10.1016/j.conb.2022.102591

Kelemen B., Pinto S., Kim N., Lisztes E., Hanyicska M., Vladar A., Olah A., Penzes Z., Shu B., Vriens J., Biro T., Rohacs T., Voets T., Toth B. I 2021) **The TRPM3 ion channel mediates nociception but not itch evoked by endogenous pruritogenic mediators** *Biochem Pharmacol* **183**:114310 https://doi.org/10.1016/j.bcp.2020.114310

Kwon D. H., Zhang F., Suo Y., Bouvette J., Borgnia M. J., Lee S 2021) **Heat-dependent opening of TRPV1 in the presence of capsaicin** *Nat Struct Mol Biol* **28**:554–563 https://doi.org/10.1038/s41594-021-00616-3

Lamming D. W., Ye L., Sabatini D. M., Baur J. A 2013) **Rapalogs and mTOR inhibitors as anti-aging therapeutics** *J Clin Invest* **123**:980–989 https://doi.org/10.1172/JCI64099

Lashinger E. S., Steiginga M. S., Hieble J. P., Leon L. A., Gardner S. D., Nagilla R., Davenport E. A., Hoffman B. E., Laping N. J., Su X 2008) **AMTB, a TRPM8 channel blocker: evidence in rats for activity in overactive bladder and painful bladder syndrome** *Am J Physiol Renal Physiol* **295**:F803–810 https://doi.org/10.1152/ajprenal.90269.2008

Liu B., Fan L., Balakrishna S., Sui A., Morris J. B., Jordt S. E 2013) **TRPM8 is the principal mediator of menthol-induced analgesia of acute and inflammatory pain** *Pain* **154**:2169–2177 https://doi.org/10.1016/j.pain.2013.06.043

Mahieu F., Janssens A., Gees M., Talavera K., Nilius B., Voets T 2010) **Modulation of the cold-activated cation channel TRPM8 by surface charge screening** *J Physiol* **588**:315–324 https://doi.org/10.1113/jphysiol.2009.183582

Malkia A, Pertusa M, Fernández-Ballester G, Ferrer-Montiel A, Viana F 2009) **Differential Role of the Menthol-Binding Residue Y745 in the Antagonism of Thermally Gated TRPM8 Channels** *Mol Pain* **5**:1744–8069 https://doi.org/10.1186/1744-8069-5-62

McCormack F. X., Inoue Y., Moss J., Singer L. G., Strange C., Nakata K., Barker A. F., Chapman J. T., Brantly M. L., Stocks J. M., Brown K. K., Lynch J. P., Goldberg H. J., Young L. R., Kinder B. W., Downey G. P., Sullivan E. J., Colby T. V., McKay R. T., ..., Group M. T. 2011) **Efficacy and safety of sirolimus in lymphangioleiomyomatosis** *N Engl J Med* **364**:1595–1606 https://doi.org/10.1056/NEJMoa1100391

McKemy D. D., Neuhausser W. M., Julius D 2002) **Identification of a cold receptor reveals a general role for TRP channels in thermosensation** *Nature* **416**:52–58 https://doi.org/10.1038/nature719

Meyer B., Peters T 2003) **NMR spectroscopy techniques for screening and identifying ligand binding to protein receptors** *Angew Chem Int Ed Engl* **42**:864–890 https://doi.org/10.1002/anie.200390233

Morice M. C., Serruys P. W., Sousa J. E., Fajadet J., Ban Hayashi E., Perin M., Colombo A., Schuler G., Barragan P., Guagliumi G., Molnar F., Falotico R., Lesions R. 2002) **A randomized comparison of a sirolimus-eluting stent with a standard stent for coronary revascularization** *N Engl J Med* **346**:1773–1780 https://doi.org/10.1056/NEJMoa012843

Muthuswamy S. K., Gilman M., Brugge J. S 1999) **Controlled dimerization of ErbB receptors provides evidence for differential signaling by homo- and heterodimers** *Mol Cell Biol* **19**:6845–6857 https://doi.org/10.1128/MCB.19.10.6845

Ochoa S. V., Casas Z., Albarracin S. L., Sutachan J. J., Torres Y. P 2023) **Therapeutic potential of TRPM8 channels in cancer treatment** *Front Pharmacol* **14**:1098448 https://doi.org/10.3389/fphar.2023.1098448

Ormerod A. D., Shah S. A., Copeland P., Omar G., Winfield A 2005) **Treatment of psoriasis with topical sirolimus: preclinical development and a randomized, double-blind trial** *Br J Dermatol* **152**:758–764 https://doi.org/10.1111/j.1365-2133.2005.06438.x

Palchevskyi S, Czarnocki-Cieciura M, Vistoli G, Gervasoni S, Nowak E, Beccari AR, Nowotny M, Talarico C 2023) **Structure of human TRPM8 channel** *Commun Biol* **6**:1–11 https://doi.org/10.1038/s42003-023-05425-6

Palkar R., Ongun S., Catich E., Li N., Borad N., Sarkisian A., McKemy D. D 2018) **Cooling Relief of Acute and Chronic Itch Requires TRPM8 Channels and Neurons** *J Invest Dermatol* **138**:1391–1399 https://doi.org/10.1016/j.jid.2017.12.025

Paricio-Montesinos R., Schwaller F., Udhayachandran A., Rau F., Walcher J., Evangelista R., Vriens J., Voets T., Poulet J. F. A., Lewin G. R. 2020) **The Sensory Coding of Warm Perception** *Neuron* **106**:830–841 https://doi.org/10.1016/j.neuron.2020.02.035

Peier A. M., Moqrich A., Hergarden A. C., Reeve A. J., Andersson D. A., Story G. M., Earley T. J., Dragoni I., McIntyre P., Bevan S., Patapoutian A 2002) **A TRP channel that senses cold stimuli and menthol** *Cell* **108**:705–715 https://doi.org/10.1016/s0092-8674(02)00652-9

Plaza-Cayón A, González-Muñiz R, Martín-Martínez M 2022) **Mutations of TRPM8 channels: Unraveling the molecular basis of activation by cold and ligands** *Medicinal Research Reviews* **42**:2168–2203 https://doi.org/10.1002/med.21920

Rohacs T., Lopes C. M., Michailidis I., Logothetis D. E 2005) **PI(4,5)P2 regulates the activation and desensitization of TRPM8 channels through the TRP domain** *Nat Neurosci* **8**:626–634 https://doi.org/10.1038/nn1451

Selvarani R., Mohammed S., Richardson A 2021) **Effect of rapamycin on aging and age-related diseases-past and future** *Geroscience* **43**:1135–1158 https://doi.org/10.1007/s11357-020-00274-1

Soria A., Agbo-Godeau S., Taieb A., Frances C 2009) **Treatment of refractory oral erosive lichen planus with topical rapamycin: 7 cases** *Dermatology* **218**:22–25 https://doi.org/10.1159/000172830

Suh B. C., Inoue T., Meyer T., Hille B 2006) **Rapid chemically induced changes of PtdIns(4,5)P2 gate KCNQ ion channels** *Science* **314**:1454–1457 https://doi.org/10.1126/science.1131163

Swarbrick A. W., Frederiks A. J., Foster R. S 2021) **Systematic review of sirolimus in dermatological conditions** *Australas J Dermatol* **62**:461–469 https://doi.org/10.1111/ajd.13671

Trepanier D. J., Gallant H., Legatt D. F., Yatscoff R. W 1998) **Rapamycin: distribution, pharmacokinetics and therapeutic range investigations: an update** *Clin Biochem* **31**:345–351 https://doi.org/10.1016/s0009-9120(98)00048-4

Vandewauw I., De Clercq K., Mulier M., Held K., Pinto S., Van Ranst N., Segal A., Voet T., Vennekens R., Zimmermann K., Vriens J., Voets T. 2018) **A TRP channel trio mediates acute noxious heat sensing** *Nature* **555**:662–666 https://doi.org/10.1038/nature26137

Varnai P., Thyagarajan B., Rohacs T., Balla T 2006) **Rapidly inducible changes in phosphatidylinositol 4,5-bisphosphate levels influence multiple regulatory functions of the lipid in intact living cells** *J Cell Biol* **175**:377–382 https://doi.org/10.1083/jcb.200607116

Vezina C., Kudelski A., Sehgal S. N 1975) **Rapamycin (AY-22,989), a new antifungal antibiotic. I. Taxonomy of the producing streptomycete and isolation of the active principle** *J Antibiot (Tokyo)* **28**:721–726 https://doi.org/10.7164/antibiotics.28.721

Voets T., Droogmans G., Wissenbach U., Janssens A., Flockerzi V., Nilius B 2004) **The principle of temperature-dependent gating in cold- and heat-sensitive TRP channels** *Nature* **430**:748–754 https://doi.org/10.1038/nature02732

Voets T., Owsianik G., Janssens A., Talavera K., Nilius B 2007) **TRPM8 voltage sensor mutants reveal a mechanism for integrating thermal and chemical stimuli** *Nat Chem Biol* **3**:174–182 https://doi.org/10.1038/nchembio862

Vriens J., Nilius B., Voets T 2014) **Peripheral thermosensation in mammals** *Nat Rev Neurosci* **15**:573–589 https://doi.org/10.1038/nrn3784

Winstein S., Henderson R. B 1943) **The Role of Neighboring Groups in Replacement Reactions. VII. The Methoxyl Group** *J. Am. Chem. Soc* **65**:2196–2200

Xiao B., Dubin A. E., Bursulaya B., Viswanath V., Jegla T. J., Patapoutian A 2008) **Identification of transmembrane domain 5 as a critical molecular determinant of menthol sensitivity in mammalian TRPA1 channels** *J Neurosci* **28**:9640–9651 https://doi.org/10.1523/JNEUROSCI.2772-08.2008

Xu L., Han Y., Chen X., Aierken A., Wen H., Zheng W., Wang H., Lu X., Zhao Z., Ma C., Liang P., Yang W., Yang S., Yang F 2020) **Molecular mechanisms underlying menthol binding and activation of TRPM8 ion channel** *Nat Commun* **11**:3790 https://doi.org/10.1038/s41467-020-17582-x

Yin Y., Le S. C., Hsu A. L., Borgnia M. J., Yang H., Lee S. Y 2019) **Structural basis of cooling agent and lipid sensing by the cold-activated TRPM8 channel** *Science* **363**:6430 https://doi.org/10.1126/science.aav9334

Yin Y., Wu M., Zubcevic L., Borschel W. F., Lander G. C., Lee S. Y 2018) **Structure of the cold- and menthol-sensing ion channel TRPM8** *Science* **359**:237–241 https://doi.org/10.1126/science.aan4325

Yin Y., Zhang F., Feng S., Butay K. J., Borgnia M. J., Im W., Lee S. Y 2022) **Activation mechanism of the mouse cold-sensing TRPM8 channel by cooling agonist and PIP(2)** *Science* **378**:eadd1268 https://doi.org/10.1126/science.add1268

Zhang X., Chen W., Gao Q., Yang J., Yan X., Zhao H., Su L., Yang M., Gao C., Yao Y., Inoki K., Li D., Shao R., Wang S., Sahoo N., Kudo F., Eguchi T., Ruan B., Xu H 2019) **Rapamycin directly activates lysosomal mucolipin TRP channels independent of mTOR** *PLoS Biol* **17**:e3000252 https://doi.org/10.1371/journal.pbio.3000252

Zhao C., Xie Y., Xu L., Ye F., Xu X., Yang W., Yang F., Guo J 2022) **Structures of a mammalian TRPM8 in closed state** *Nat Commun* **13**:3113 https://doi.org/10.1038/s41467-022-30919-y

Author information

Balázs István Tóth*

Laboratory of Cellular and Molecular Physiology, Department of Physiology, Faculty of Medicine, University of Debrecen, Debrecen, Hungary, Laboratory of Ion Channel Research, Department of Cellular and Molecular Medicine, KU Leuven, Leuven, Belgium

ORCID iD: 0000-0002-4103-4333

For correspondence: toth.istvan@med.unideb.hu

*These authors contributed equally

Bahar Bazeli*
Laboratory of Ion Channel Research, Department of Cellular and Molecular Medicine, KU Leuven, Leuven, Belgium, VIB Center for Brain & Disease Research, Leuven, Belgium
ORCID iD: 0000-0001-9568-2689

*These authors contributed equally

Annelies Janssens
Laboratory of Ion Channel Research, Department of Cellular and Molecular Medicine, KU Leuven, Leuven, Belgium, VIB Center for Brain & Disease Research, Leuven, Belgium
ORCID iD: 0000-0002-6735-8248

Erika Lisztes
Laboratory of Cellular and Molecular Physiology, Department of Physiology, Faculty of Medicine, University of Debrecen, Debrecen, Hungary
ORCID iD: 0000-0002-8517-6536

Márk Racskó
Laboratory of Cellular and Molecular Physiology, Department of Physiology, Faculty of Medicine, University of Debrecen, Debrecen, Hungary, Doctoral School of Molecular Medicine, Faculty of Medicine, University of Debrecen, Debrecen, Hungary

Balázs Kelemen
Laboratory of Cellular and Molecular Physiology, Department of Physiology, Faculty of Medicine, University of Debrecen, Debrecen, Hungary, Laboratory of Ion Channel Research, Department of Cellular and Molecular Medicine, KU Leuven, Leuven, Belgium
ORCID iD: 0000-0002-8994-0132

Mihály Herczeg
Department of Pharmaceutical Chemistry, University of Debrecen, Debrecen, Hungary
ORCID iD: 0000-0002-7938-9789

Tamás Milán Nagy
MTA-DE Molecular Recognition and Interaction Research Group, University of Debrecen, Debrecen, Hungary, Department of Chemistry, University of Umeå, Umeå, Sweden
ORCID iD: 0000-0003-4766-1992

Katalin E Kövér
MTA-DE Molecular Recognition and Interaction Research Group, University of Debrecen, Debrecen, Hungary, Department of Inorganic and Analytical Chemistry, University of Debrecen, Debrecen, Hungary
ORCID iD: 0000-0001-5020-4456

Argha Mitra
Laboratory of Chemical Biology, Institute of Biochemistry, HUN-REN Biological Research Centre, Szeged, Hungary, Theoretical Medicine Doctoral School, Faculty of Medicine, University of Szeged, Szeged, Hungary
ORCID iD: 0000-0002-5497-1975

Attila Borics
Laboratory of Chemical Biology, Institute of Biochemistry, HUN-REN Biological Research Centre, Szeged, Hungary
ORCID iD: 0000-0002-6331-3536

Tamás Bíró
Department of Immunology, Faculty of Medicine, University of Debrecen, Debrecen, Hungary
ORCID iD: 0000-0002-3770-6221

Thomas Voets
Laboratory of Ion Channel Research, Department of Cellular and Molecular Medicine, KU Leuven, Leuven, Belgium, VIB Center for Brain & Disease Research, Leuven, Belgium
ORCID iD: 0000-0001-5526-5821

For correspondence: thomas.voets@kuleuven.be

Editors

Reviewer #1 (Public review):

Summary:

In this valuable study, the authors found that the macrolide drug rapamycin, which is an important pharmacological tool in the clinic and the research lab, is less specific than previously thought. They provide solid functional evidence that rapamycin activates TRPM8 and begin to develop an NMR method to measure the specific binding of a ligand to a membrane protein.

Strengths:

The authors use a variety of complementary experimental techniques in several different systems, and their results support the conclusions drawn.

Weaknesses:

The proposed location of the rapamycin binding pocket within the membrane means that molecular docking approaches designed for soluble proteins alone do not provide solid evidence for a rapamycin binding pocket location in TRPM8, but the authors are appropriately careful in stating that the model is consistent with their functional experiments. The novel STTD method is intriguing and supportive of the functional results and docking predictions, but further validation of this method is needed.

Impact:

This work provides still more evidence for the polymodality of TRP channels, reminding both TRP channel researchers and those who use rapamycin in other contexts that the adjective "specific" is only meaningful in the context of what else has been explicitly tested.

Comments on revisions:

The authors have addressed my major concerns from the previous round of revision, and I agree that those things that remain un-done are outside the scope of this manuscript.

https://doi.org/10.7554/eLife.97341.2.sa3

Reviewer #2 (Public review):

Summary:

Tóth and Bazeli et al. find rapamycin activates heterologously-expressed TRPM8 and dissociated sensory neurons in a TRPM8-dependent way with Ca2+-imaging. With electrophysiology and STTD-NMR, they confirmed the activation is through direct interaction with TRPM8. Using mutants and computational modeling, the authored localized the binding site to the groove between S4 and S5, different than the binding pocket of cooling agents such as menthol. The hydroxyl group on carbon 40 within the cyclohexane ring in rapamycin is indispensable for activation, while other rapalogs with its replacement, such as everolimus, still bind but cannot activate TRPM8. Overall, the findings provide new insights into TRPM8 functions and may indicate previously-unknown physiological effects or therapeutic mechanisms of rapamycin.

Strengths:

The authors spent extensive effort on demonstration that the interaction between TRPM8 and rapamycin is direct. The evidence is solid. In probing the binding site and the structural-function relationship, the authors combined computational simulation and functional experiments. It is very impressive to see that "within" a rapamycin molecule, the portion shared with everolimus is for "binding", while the hydroxyl group in the cyclohexane ring is for activation. Such detailed dissection represents a successful trial in computational biology-facilitated, functional experiment-validated study of TRP channel structural-activity relationship. The research draws the attention of scientists, including those outside the TRP channel field, to previously-neglected effects of rapamycin, and therefore the manuscript deserves broad readership.

Weaknesses:

The significance of the research could be improved by showing or discussing whether a similar binding pocket is present in other TRP channels, and hence rapalogs might bind to or activate these TRP channels. Additionally, while the finding on TRPM8 is novel, it is worthwhile to perform more comprehensive pharmacological characterization, including single-channel recording and a few more mutant studies to offer further insight into the mechanism of rapamycin binding to S4~S5 pocket driving channel opening. It is also necessary to know if rapalogs have independent or synergistic effects on top of other activators, including cooling agents and lower temperature, and its dependence on regulators such as PIP2.

Additional discussion that might be helpful:

The authors did confirm that rapamycin does not activate TRPV1, TRPA1 and TRPM3. But other TRP channels, particularly other structurally-similar TRPM channels, should be discussed or tested. Alignment of the amino acid sequences or structures at the predicted binding pocket might predict some possible outcomes. In particular, rapamycin is known to activate TRPML1 in a PI(3,5)P2-dependent manner, which should be highlighted in comparison among TRP channels (PMID: 35131932, 31112550).

After revision:

I acknowledge that the authors have addressed some of the questions in their revised version. They have explained that additional experiments might be beyond the scope of the current study. I appreciate their effort in doing their best to improve the manuscript and to leave the rest in discussion.

https://doi.org/10.7554/eLife.97341.2.sa2

Reviewer #3 (Public review):

Summary:

Rapamycin is a macrolide of immunologic therapeutic importance, proposed as a ligand of mTOR. It is also employed as in essays to probe protein-protein interactions.
The authors serendipitously found that the drug rapamycin and some related compounds, potently activate the cationic channel TRPM8, which is the main mediator of cold sensation in mammals. The authors show that rapamycin might bind to a novel binding site that is different from the binding site for menthol, the prototypical activator of TRPM8. These convincing results are important to a wide audience, since rapamycin is a widely used drug and is also employed in essays to probe protein-protein interactions, which could be affected by potential specific interactions of rapamycin with other membrane proteins, as illustrated herein.

Strengths:

The authors employ several experimental approaches to convincingly show that rapamycin activates directly the TRPM8 cation channel and not an accessory protein or the surrounding membrane. In general, the electrophysiological, mutational and fluorescence imaging experiments are adequately carried out and cautiously interpreted, presenting a clear picture of the direct interaction with TRPM8. In particular, the authors convincingly show that the interactions of rapamycin with TRPM8 are distinct from interactions of menthol with the same ion channel.

Weaknesses:

The main weakness of the manuscript was the NMR method employed to show that rapamycin binds to TRPM8. The authors developed and deployed a novel signal processing approach based on subtraction of several independent NMR spectra to show that rapamycin binds to the TRPM8 protein and not to the surrounding membrane or other proteins. In this revised version the authors have strengthened the evidence that the method gives solid results and have improved the clarity of the presentation.

Comments on revisions:

The authors have greatly improved the quality of the presentation of the NMR data and have answered my concerns regarding the new methodology. The manuscript is improved and represents an important contribution.

https://doi.org/10.7554/eLife.97341.2.sa1

Author response:

The following is the authors' response to the original reviews.

Public Reviews:

Reviewer #1 (Public Review):

Summary:

In this valuable study, the authors found that the macrolide drug rapamycin, which is an important pharmacological tool in the clinic and the research lab, is less specific than previously thought. They provide solid functional evidence that rapamycin activates TRPM8 and develop an NMR method to measure the specific binding of a ligand to a membrane protein.

Strengths:

The authors use a variety of complementary experimental techniques in several different systems, and their results support the conclusions drawn.

Weaknesses:

Controls are not shown in all cases, and a lack of unity across the figures makes the flow of the paper disjointed. The proposed location of the rapamycin binding pocket within the membrane means that molecular docking approaches designed for soluble proteins alone do not provide solid evidence for a rapamycin binding pocket location in TRPM8, but the authors are appropriately careful in stating that the model is consistent with their functional experiments.

Impact:

This work provides still more evidence for the polymodality of TRP channels, reminding both TRP channel researchers and those who use rapamycin in other contexts that the adjective "specific" is only meaningful in the context of what else has been explicitly tested.

Reviewer #2 (Public Review):

Summary:

Tóth and Bazeli et al. find rapamycin activates heterologously-expressed TRPM8 and dissociated sensory neurons in a TRPM8-dependent way with Ca2+-imaging. With electrophysiology and STTD-NMR, they confirmed the activation is through direct interaction with TRPM8. Using mutants and computational modeling, the authored localized the binding site to the groove between S4 and S5, different than the binding pocket of cooling agents such as menthol. The hydroxyl group on carbon 40 within the cyclohexane ring in rapamycin is indispensable for activation, while other rapalogs with its replacement, such as everolimus, still bind but cannot activate TRPM8. Overall, the findings provide new insights into TRPM8 functions and may indicate previously unknown physiological effects or therapeutic mechanisms of rapamycin.

Strengths:

The authors spent extensive effort on demonstrating that the interaction between TRPM8 and rapamycin is direct. The evidence is solid. In probing the binding site and the structural-function relationship, the authors combined computational simulation and functional experiments. It is very impressive to see that "within" a rapamycin molecule, the portion shared with everolimus is for "binding", while the hydroxyl group in the cyclohexane ring is for activation. Such detailed dissection represents a successful trial in the computational biology-facilitated, functional experiment-validated study of TRP

channel structuralactivity relationship. The research draws the attention of scientists, including those outside the TRP channel field, to previously neglected effects of rapamycin, and therefore the manuscript deserves broad readership.

Weaknesses:

The significance of the research could be improved by showing or discussing whether a similar binding pocket is present in other TRP channels, and hence rapalogs might bind to or activate these TRP channels. Additionally, while the finding on TRPM8 is novel, it is worthwhile to perform more comprehensive pharmacological characterization, including single-channel recording and a few more mutant studies to offer further insight into the mechanism of rapamycin binding to S4~S5 pocket driving channel opening. It is also necessary to know if rapalogs have independent or synergistic effects on top of other activators, including cooling agents and lower temperature, and their dependence on regulators such as PIP2.

Additional discussion that might be helpful:

The authors did confirm that rapamycin does not activate TRPV1, TRPA1 and TRPM3. But other TRP channels, particularly other structurally similar TRPM channels, should be discussed or tested. Alignment of the amino acid sequences or structures at the predicted binding pocket might predict some possible outcomes. In particular, rapamycin is known to activate TRPML1 in a PI(3,5)P2-dependent manner, which should be highlighted in comparison among TRP channels (PMID: 35131932, 31112550).

Reviewer #3 (Public Review):

Summary:

Rapamycin is a macrolide of immunologic therapeutic importance, proposed as a ligand of mTOR. It is also employed as in essays to probe protein-protein interactions.

The authors serendipitously found that the drug rapamycin and some related compounds, potently activate the cationic channel TRPM8, which is the main mediator of cold sensation in mammals. The authors show that rapamycin might bind to a novel binding site that is different from the binding site for menthol, the prototypical activator of TRPM8. These solid results are important to a wide audience since rapamycin is a widely used drug and is also employed in essays to probe protein-protein interactions, which could be affected by potential specific interactions of rapamycin with other membrane proteins, as illustrated herein.

Strengths:

The authors employ several experimental approaches to convincingly show that rapamycin activates directly the TRPM8 cation channel and not an accessory protein or the surrounding membrane. In general, the electrophysiological, mutational and fluorescence imaging experiments are adequately carried out and cautiously interpreted, presenting a clear picture of the direct interaction with TRPM8. In particular, the authors convincingly show that the interactions of rapamycin with TRPM8 are distinct from interactions of menthol with the same ion channel.

Weaknesses:

The main weakness of the manuscript is the NMR method employed to show that rapamycin binds to TRPM8. The authors developed and deployed a novel signal processing approach based on subtraction of several independent NMR spectra to show that rapamycin binds to the TRPM8 protein and not to the surrounding membrane or other proteins. While interesting and potentially useful, the method is not well developed

> *(several positive controls are missing) and is not presented in a clear manner, such that the quality of data can be assessed and the reliability and pertinence of the subtraction procedure evaluated.*
>
> ***Recommendations for the authors:***
>
> ***Reviewer #1 (Recommendations For The Authors):***
>
> *Major points*
>
> *(1) Given the novelty of the STTD NMR approach, please provide more details and data for the reader.*
>
> *• I would like to see all of the collected spectra so that readers can see and judge the effect sizes for themselves, perhaps as an additional supplementary figure.*

We agree with the reviewer that the data transparency of the NMR measurements should be improved. We changed panel C of Figure 2 in the main text and provided all the STD and the computed STDD and STTD spectra recorded on one set of experiments. We carried out additional experimental replicas on new samples and addressed the variability of cell samples by rescaling the STD effects based on reference ^{1}H measurements. We provided supplementary spectra of the reference experiments without saturation (Figure S5) and the obtained STTD spectra from the three parallel NMR sessions (Figure S6).

> *• I appreciate the labels for STDD-1, STDD-2, and STTD on the lower two spectra of Figure 2C. Is the top spectrum from STD-1 or is it prior to saturation? In Figure 2C, what do the x1 and x2 notations on the right-hand side of the spectra indicate?*

We showed the top spectrum as an overview and a demonstration of the spectral complexity of the samples. ^{1}H experiments were run before the STD measurements to assess the sample quality and stability. The demonstrated spectrum on sample 1 (TRPM8 with rapamycin in HEK cells) was recorded with more transients than the corresponding STDs, thus it is only visually comparable with the difference spectra after scaling (2x). Figure 2 was changed and all the spectra were replaced as mentioned before. All the recorded ^{1}H-experiments without saturation including the one removed are now available in the supplementary information (Figure S5).

> *• The STTD NMR results with WT TRPM8 are consistent with rapamycin binding directly to the channel. Testing whether rapamycin binding observed with STTD NMR is disrupted by one of the most compelling mutations (D796A, D802A, G805A, or Q861A) would be a further test of this direct interaction.*

We thank the reviewer for the suggestion and agree that testing the most compelling mutants would be a promising next step. These mutations were generated in plasmid vectors and only transiently transfected into HEK cells. For NMR analysis we would need a high amount of cells stably overexpressing the mutant channels which were not available for experimentation.

> *• Given that this is not a methods paper, it is probably outside the scope to further validate the STTD NMR measurements by performing parallel ITC, SPR, MST, or radiolabeled ligand experiments. Nevertheless, I would be excited to see such a comparison since STTD NMR appears to have promise as an experimental technique for assessing ligand binding to membrane proteins that does not require large amounts of purified protein or radioactive isotopes.*

We agree with the reviewer that additional independent biophysical measurements on the interactions are necessary to further validate the STTD methodology. This paper is a preliminary demonstration of the STTD concept and our group is currently working on the challenges of on-cell NMR (e.g., sample and spectral complexity) and the standardization of the proposed workflow.

> *(2) Please clarify the methods used to model of rapamycin binding. Docking can be imprecise in TRP channels, even with a sophisticated docking scheme (Hughes et al., 2019, doi: https://doi.org/10.7554/eLife.49572.001).*

Thank you for mentioning this point and providing the reference. We have further clarified our methods and included the reference in our discussion, indicating the limitations of our approach.

> *• As a positive control, does the docking strategy accurately predict binding of known compounds (menthol, icilin, etc.) to TRPM8 consistent with cryo-EM structures?*

Yes, the binding site for menthol, based on a similar docking strategy as for rapamycin, is also presented, and matches with predictions from other publications. This is now clarified in the revised manuscript.

> *• Why was homology modeling to the human sequence used with the mouse structure but not the avian structure?*

At this onset of the project, only the avian structure was available, and it was used in the primary docking. Later, to get more precise docking relevant for human TRPM8 pharmacology, we did revert to the then available structure of the mouse ortholog.

> *• How many rapamycin structural clusters were built, and how many structures were there in each cluster? How many were used? "most populated" is unspecific.*

Thank you for your comment. We have added the following highlighted information to the methods section to address your comment:

“Representative conformations of rapamycin were identified by clustering of the 1000-membered pools, having the macrocycle backbone atoms compared with 1.0 Å RMSD cut-off. Middle structures of the ten most populated clusters, accounting for more than 90% of the total conformational ensemble generated by simulated annealing, were used for further docking studies. To refine initial docking results and to identify plausible binding sites, the above selected rapamycin structures were docked again, following the same protocol as above, except for the grid spacing which was set to 0.375 Å in the second pass. The resultant rapamycin-TRPM8 complexes were, again, clustered and ranked according to the corresponding binding free energies. Selected binding poses were subjected to further refinement. The three most populated and plausible binding poses were further refined by a third pass of docking, where amino acid side chains of TRPM8, identified in the previous pass to be in close contact with rapamycin (< 4 Å), were kept flexible. Grid volumes were reduced to these putative binding sites including all flexible amino acid side chains (21.0-26.2 Å x 26.2-31.5 Å x 24.8-29.2 Å).”

However, it is important to clarify that the clusters are not built and their number is not specified by the user. The number of clusters found depends on how similar the structures are in the structural ensemble analyzed by clustering. A high number of clusters indicates a diverse, whereas a low number suggests a uniform structural ensemble. Furthermore, it is arbitrarily controlled by the similarity cutoff specified by the user. If the cutoff is selected

well, then the number of structures is different in each cluster. There are some highly populated clusters and a few which only have one structure. The selection of how many cluster representatives are used is usually based on the decision of whether or not the sum of the population of selected clusters sufficiently covers the mapped conformational space.

> *• Additionally, the rapamycin poses were generated using a continuum solvent model that is unlikely to replicate the conditions existing in the lipid bilayer or in a lipid-exposed binding pocket as is predicted here. It is therefore possible that the rapamycin poses chosen for docking do not represent the physiological rapamycin binding pose, hampering the ability of the docking algorithm to find an appropriate docking pocket.*
>
> *• Furthermore, accurately docking that may bind to membrane-exposed pockets is a challenging problem, particularly because many scoring algorithms, including those employed by Autodock, do not distinguish between solvent-exposed and membrane-exposed faces of the protein. This affects the predicted binding energies.*

We appreciate the reviewer's insightful comments. We add a note in discussion part, mentioning these important limitations.

> *• In Figure 4, it appears that the proposed rapamycin binding pocket is located at the interface between two subunits, but only one is shown. Is there any contact with residues in the neighboring subunit? Based on Figure S4, I assume not, but am unsure.*

Based on the estimated distances, we do not think that there are any relevant interactions with residues from neighboring subunits. This is now indicated in the results section.

> *• Consider uploading the rapamycin-docked model to a public repository such as Zenodo for readers to examine and manipulate themselves*

As suggested, the model will be uploaded in a public repository. A link to the file on Zenodo is now included.

> *(3) Please discuss the spatial location of the proposed rapamycin binding pocket relative to the vanilloid binding pocket in TRPV1.*
>
> *• The mutagenesis indicates that D745, D802, G805, and Q861 are most important for rapamycin sensitivity in TRPM8. Interestingly, the proposed rapamycin binding pocket appears to overlap spatially with the vanilloid binding pocket in TRPV1. Consistent with this, Q861 aligns with E570 in TRPV1, which is a critical residue for resiniferatoxin sensitivity. Indeed, similar to Q861's modeled proximity to the cyclohexyl ring, the hydroxyl group of the vanillyl moity of capsaicin (4DY in 7LR0, for example) is in proximity to E750 in TRPV1. Additionally, searching PubChem by structural similarity suggests that vanillyl head group of the TRP channel modulators capsaicin and eugenol are similar structurally to the trans-2Methoxycyclohexan-1-ol ring. Without overlaying the two structures myself, it is difficult to say more than that, but I encourage the authors to comment on any similarities and differences they observe.*
>
> *• If the proposed rapamycin pocket is indeed similar to the location of the vanilloid binding site, the authors may wish to discuss other TRPM channel structures that show ligands and lipids bound to this pocket because this provides evidence that this pocket influences TRPM channel function. For example, how does the proposed rapamycin binding pocket compare to TRPM8 bound to agonist AITC (PDBID 8e4l), TRPM5 bound to inhibitor NDNA (7mbv), and TRPM2 bound to phosphatidylcholine (6co7)?*

> *• Other TRP channel structures with ligands or lipids modeled in this region include TRPV1 bound to resiniferatoxin, capsaicin, or phosphatidylinositol (7l2j, 7l24, 7l2s, 7l2t, 7l2u, 7lp9, 7lpc, 7lqy, 7mz6, 7mz9, 7mza); TRPV3 bound to phosphatidylcholine (7mij, 7mik, 7mim, 7min, 7ugg); TRPV5 bound to econazole (6b5v) or ZINC9155 (6pbf); TRPV6 bound to piperazine (7d2k, 7k4b, 7k4c, 7k4d, 7k4e, 7k4f) or cholesterol hemisuccinate (7s8c); TRPC6 bound to BTDM (7dxf) or phosphatidylcholine (6uza); and TRP1 bound to PIP2 (6pw5).*

We thank the reviewer for these valuable insights. We have included some additional discussion highlighting the similarities between the proposed rapamycin binding site and some of the other ligandchannel interactions in the TRP superfamily, in particular the well-known vanilloid binding site in TRPV1. However, to keep the discussion focused, we have not fully discussed all the indicated interactions, to best serve the clarity and scope of the manuscript.

> *(4) I would like to see negative control calcium imaging and electrophysiology data with untransfected HEK cells to confirm that the observed activation is mediated by TRPM8 to parallel the TRPM8 KO sensory neuron experiments.*

This important information is now included in the revised manuscript (Figure S2).

> *(5) The DM-nitrophen Ca uncaging experiments are an interesting method to test Ca sensitivity of rapamycin, but the results make these experiments more complex to interpret. Ca has been shown to be an obligate cofactor for icilin sensitivity in TRPM8 under conditions where both the internal and external Ca concentrations are tightly controlled (Kuhn et al., 2009, doi: https://doi.org/10.1074/jbc.M806651200), which is necessary because TRPM8 allows Ca permeation through the pore when open. The large icilin-evoked currents in Figure 5A and 5B indicate that the effective intracellular calcium concentration is not zero prior to calcium uncaging, which may be high enough to mask any Ca-dependence of rapamycin that occurs at low Ca concentrations. Given this ambiguity, the inside-out patch clamp configuration would provide more control over the internal and external Ca concentration than is achieved in the Ca uncaging experiments. Because the authors have already demonstrated their ability to perform such experiments (Figure 2 panel B), it would be nice to see tests of Ca dependence using inside-out patch clamp.*

As was already shown in Figure 2, Rapamycin activates TRPM8 in inside-out patches, and these experiments were performed using calcium-free cytosolic and extracellular solutions. Note that earlier studies have already shown that icilin activates outward TRPM8 currents in the full absence of calcium: see e.g. Janssens et al. eLife, 2016. Chuang et al. 2004. In the case of Icilin, increased calcium further potentiates the current, which is more prominent for the inward current.

In the Ca uncaging experiments, considering the Kd of DM-nitrophen of 5 nM, we expect that the intracellular calcium concentration before the UV flash would be approximately 15 nM. Taken together, both the inside-out experiments and the flash uncaging experiments confirm that rapamycin responses are not directly regulated by intracellular calcium, contrary to icilin.

> *(6) Sequence conservation within TRPM channels could be used in combination with the binding pocket model and mutagenesis to predict rapamycin selectivity for TRPM8 over other TRPMs. For example, some important residues, specifically G805 and Q861, are not conserved in TRPM3, which agrees with the lack of rapamycin sensitivity observed in TRPM3 (Figure S1). Further sequence comparison would provide testable hypotheses for*

> *future exploration of rapamycin sensitivity in other TRPMs that could validate the proposed binding pocket.*

Thank you for the suggestion. We now indicate in the discussion that only some of the key residues are conserved and make suggestions for future studies.

> *(7) Please unify the color scheme across the figures to improve clarity.*
>
> *• The authors frequently use the colors blue, red, and green to represent menthol and rapamycin in the figures, but they are inconsistent in which one represents menthol and which represents rapamycin. It would be clearer for the audience if, for example, rapamycin is always represented with red and menthol is always represented with blue.*

Thank you for pointing this out. We have made the coloring schemes more uniform.

> *• In Figure 1, panel E, the coloring for Menthol and Pregnenolone Sulfate changes between the TRPM8+/+ and TRPM8-/- panels.*

Thank you for pointing this out. We have updated the coloring schemes to ensure consistency between the TRPM8+/+ and TRPM8-/- panels.

> *• Figure 3 B and E, perhaps color the plot background as a 3-color gradient (blue to white to red) rather than yellow and aqua. Center the white at the WT ratio, keeping the dashed line, with diverging gradients to, for example, blue for mutations that selectively affect menthol sensitivity and red for rapamycin.*

Thank you for the suggestion – we have changed the figure accordingly.

> *• Figure 4 panels A and B use the same color (green) to show two different things (menthol molecule and mutated residues that affect rapamycin sensitivity). It would be clearer for readers to change these colors to agree with a unified color scheme such that, for example, the menthol molecule is colored blue and the rapamycin-neighboring residues are colored red.*

Thank you for the suggestion. We have updated the figure to use a unified color scheme, with the menthol molecule now colored green and the rapamycin-neighboring residues colored cyan, to enhance clarity for readers.

> *• I recommend adding a figure or panel that shows side chains for all mutations, colored by menthol/rapamycin selectivity, as indicated by the functional data in Figure 3B and 3E. This will highlight spatial patterns of the selective residues that are discussed in the text.*

Thank you for your suggestion, we added all the side residues in Figure S10.

> *Minor points*
>
> *(1) It would be nice to have one more concentration data point in the middle of the dose response curve shown in Figure 1 panel B. The response is not saturating at the top or foot of the curve in Figure 1 panel D, precluding a confident fit to a two-state Boltzmann function.*

Instead of adding a single data point to this figure, we performed independent measurements on a plate reader system, comparing concentration responses at room temperature and 37 degrees. These data are now included as Figure S1.

> *(2) The cartoon in Figure 2 panel B should be made more accurate. For example, only the transmembrane helices should be depicted embedded in the membrane, not the whole protein including the intracellular domain. Because the experiment was performed with cells, change the orientation of TRPM8 in the cartoon to show the intracellular domain of the protein facing away from the extracellular side of the membrane where the rapamycin is applied.*

Thank you for this comment. We have corrected the cartoon accordingly

> *(3) Perhaps put the yellow circles under or around the carbon atoms to which the identified hydrogen atoms belong in Figure 2 panel E and Figure 4 panel C. I found it difficult to visualize and compare the STTD NMR results with the predicted binding pocket.*

Thank you for the feedback. We have added yellow circles around the carbon atoms corresponding to the identified hydrogen atoms in Figure S9.

> *(4) Regarding the sentence on p. 12 beginning "In agreement with this notion..."*
>
> *• Include icilin, Cooling Agent-10, and WS-3 as other cooling agents whose sensitivity has been modulated by mutation of Y745*
>
> *• Cryosim-3 responses were not tested in either of the two papers cited; please add citation to Yin et al., 2022, doi: https://doi.org/10.1126/science.add1268 .*
>
> *• Other relevant papers include:*
>
> *– Malkia et al., 2009, doi: https://doi.org/10.1186/1744-8069-5-62 which includes molecular docking showing the hydroxyl group of menthol interacting with Y745*
>
> *– Beccari et al., 2017, doi: https://doi.org/10.1038/s41598-017-11194-0 Figure 5 shows disruption of icilin and Cooling Agent-10 sensitivity by Y745A*
>
> *– Palchevskyi et al., 2023, doi: https://doi.org/10.1038/s42003-023-05425-6 Figure 3 shows disruption of icilin, cooling agent-10, WS-3, and menthol sensitivity by Y745A o Plaza-Cayon et al., 2022, https://doi.org/10.1002%2Fmed.21920 Review of TRPM8 mutations*
>
> *• typo: Y754H should be Y745H*

Thank you for these suggestions. We have added the above references to the text and corrected the typo.

> *(5) The authors use the competitive action of everolimus on rapamycin activation as evidence that the different macrolides are binding to the same binding pocket. In addition, prior work showed that Y745H and N799A mutations (which render TRPM8 insensitive to menthol and icilin, respectively) do not affect TRPM8 sensitivity to the structurally-related compound tacrolimus (Arcas et al., 2019). This is consistent with the docking and mutagenesis results presented here.*

Thank you for this valuable suggestion. We discuss these data in the revised version.

> *(6) Rapamycin sensitivity has also been observed in TRPML1 (Zhang et al. 2019, doi: https://doi.org/10.1371/journal.pbio.3000252).*

We added a short reference to this interesting finding in the discussion.

> *(7) The whole-cell currents are very large in several of the electrophysiology experiments (for example Figure 3 panel D and Figure S1), which could lead to artifacts of voltage errors as well as ion accumulation/depletion. However, because this paper is not relying on reversal potential measurements or trying to quantify V1/2, these errors are unlikely to affect the qualitative conclusions drawn.*

This is a fair point, but indeed unlikely to affect our main conclusions. Note that we compensated between 70 and 90% of the series resistance, so we don't expect voltage errors exceeding ~10 mV.

> *(8) Ligand sensitivity is frequently species-dependent in TRP channels, so it is interesting that multiple species were used here and that both human and mouse isoforms exhibit rapamycin sensitivity. It should be emphasized that human TRPM8 was used in the calcium imaging and electrophysiology experiments, as well as some docking models, while the mouse isoform was used in the sensory neuron experiments and a mutated avian isoform was used for some docking models.*

This information is available in the Methods and we believe it is clear for the readers.

> *(9) Perhaps discuss the unclear mechanism of G805A action in icilin (but not menthol, cold, or praziquantel) sensitivity because it is not in direct contact with the ligand. For example, Yin et al., 2019 propose flexibility allowing Ca binding site and larger binding site for icilin.*

Yin et al. (2019) suggests that the G805A mutation impacts icilin sensitivity by influencing the flexibility of the binding site and possibly affecting calcium binding. In our study, we found that G805A significantly reduces rapamycin sensitivity, likely due to its direct role in the rapamycin binding pocket rather than affecting calcium binding. This is now briefly mentioned in the results section.

> *(10) The Figure S1 legend indicates that n=5 for all panels, so please show normalized population IV curves rather than individual examples. Additionally, it would be interesting to see what happens when each agonist is co-applied with rapamycin. Does rapamycin potentiate or inhibit agonist activation in these channels and/or TRPM8?*

We believe that normalized population IVs are not ideal for representing whole-cell currents, considering the substantial variation in current densities. We therefore prefer to show example traces in Figure S3 of the revised version but include mean values of current densities for all tested cells in the text.

While the effects of co-application of rapamycin with activating ligands could be of interest, we consider this somewhat outside the scope of the present manuscript. The combination of HEK293 cell experiments, along with results obtained in WT and TRPM8-deficient mice does, in our opinion, sufficiently describe the selectivity of rapamycin towards TRPM8 compared to other sensory TRP channels.

> *(11) Figure S1 panel A does not contain units for Rapamycin or AITC concentrations.*

Thank you for pointing this out. The units were added to the figure.

> *(12) It would be nice if the authors characterized the different mutations as predicted to contribute to site 1 (D796, H845, Q861, based on Figure S4), site 2 (D796, M801, F847,*

> *and R851), and/or site 3 (F847, V849, and R851).*

The indicated mutants were all tested, as shown in Figure 3.

> *(13) The numbering scheme in Figure S4 does not appear to match the residue numbers in the rest of the paper for certain residues (HIS-844 rather than H845, PHE-846 rather than F847, VAL-848 rather than V849, ARG-850 rather than R851, and GLN-860 rather than Q861), and labels are often overlapping and difficult to see. I also find the transparent spheres very difficult to distinguish from the transparent background, which makes it difficult to appreciate the STTD NMR data overlay.*

We apologize for the confusing numbering scheme. The lower numbers refer to the initial docking that was done using the avian TRPM8 ortholog. We have made a newer, clearer version of Figure S4 and inserted as Figure S9.

> *(14) Please superpose the Ligplots in Figure S5 panels E and F as described in the LigPlus manual (https://www.ebi.ac.uk/thornton-srv/software/LigPlus/manual/manual.html) to facilitate easier comparison.*

Thank you for the suggestion. We followed the suggestion to superpose the Ligplots as described but found that the result was visually cluttered and difficult to interpret. To avoid confusion, we instead decided to remove panels E and F from Figure S5, as we believe that the visualization in panels A-D is clear and informative.

> *(15) Some n values are missing in figure legends.*

We checked all legends, and added n numbers were missing.

> *(16) There is an inconsistent specification of error bars as SEM in the figure legends, though it is specified in methods.*
>
> *A question for my own edification: Here, you have looked at ligand interactions with the protein by saturating the protein resonances and observing transfer to the ligand. Would it be possible to instead saturate lipid or solute resonances and observe transfer to a ligand? I am curious whether this would be one way to measure equilibrium partitioning of ligand into a membrane and/or determine the effective concentration of a ligand in the membrane. Additionally, could one determine whether the compound is fully partitioned into the center of the membrane or just sitting on the surface?*

The reviewer highlights an interesting aspect. The widely used WaterLOGSY NMR experiment (doi: 10.1023/a:1013302231549) saturates water molecules then the magnetization is transferred to the ligand of interest. Characteristic changes in ligand resonances are observed in the case of a binding event with proteins. On the other hand, the selective saturation of lipids is -while theoretically possible –technically challenging mainly because of the inherent low signal-dispersion of lipids and peak overlapping with ligand resonances. Additionally, lipid systems are more dynamic compared to proteins and ligand-lipid interactions could be weaker and less specific, significantly affecting the sensitivity of STD experiments.

> ***Reviewer #2 (Recommendations For The Authors):***
>
> *Major:*
>
> *• Is it feasible to test rapamycin on TRPM8 with single-channel recording? This will allow us to better probe the mechanism of rapamycin activation and compare it with menthol, with parameters of singlechannel conductance and maximal open probability.*

In our experience, it is very difficult to obtain single-channel recordings from TRPM8. The channel expresses at high densities, typically leading to patches contain multiple channels, making a proper analysis of mean open and closed times very difficult. Therefore, we have decided not to include such measurements in the manuscript.

> *• The authors classified rapamycin as a type I agonist, the type that stabilizes the open conformation, same as menthol but more prominent. Does that indicate that rapamycin work synergistically (rather than independently) with menthol, because co-application of them can allow them to add to each other in stabilizing the open conformation? I wonder if the authors agree that this could be tested with experiments as in Figure S3, by showing a much more prolonged deactivation with co-application of menthol and rapamycin than applying each alone.*

Thank you for the insightful suggestion. We conducted co-application experiments, and our results show that the deactivation time is indeed significantly prolonged when both compounds are applied together compared to each alone. In fact, very little deactivation is seen when both compounds are co-applied, which made it virtually impossible to perform reliable fits to the deactivation time course for the Menthol+Rapamycin condition. Instead, we have now included summary results showing the percentage of deactivation after 100 ms. We included these findings in FigureS8.

> *• It could be tested whether rapamycin activation of TRPM8 requires or overrides the requirement of PIP2 with inside-out patch by briefly exposing the patch to poly-lysine to sequester PIP2.*

This is certainly a good suggestion for further follow-up studies. However, we considered that examination of the (potential) interaction between ligands and PIP2 was outside the scope of the current manuscript.

> *• Figure 1C suggests that the authors test rapamycin when there is a relatively high baseline TRPM8 activation (prior to rapamycin) activation. This raises the possibility that rapamycin is more a potentiator than an activator. I wonder if the following two experiments could address it: (1) perfuse rapamycin while holding at different membrane potentials, wash-off rapamycin in the solution and quickly (in a few seconds) test the activated current magnitude (before rapamycin dissociation), to compare whether a more depolarized membrane potential (high baseline open probability) allows rapamycin to potentiate more. (2) Perform the experiment at a higher temperature (low baseline open probability) and test whether rapamycin EC50 shifts to the right.*

Thank you for the thoughtful suggestion. Overall, we are not really in favor of making a distinction between a potentiator and an activator since it is not really feasible to create a situation where TRPM8 activity is zero. As suggested, we performed the dose response experiment at a higher temperature (37 °C) and observed that rapamycin's EC_{50} shifts to the right FigureS2. This is similar to what has been observed for menthol on TRPM8 and for many other ligands on other temperature-sensitive TRP channels.

> *Minor:*
>
> *(1) The author should report hill coefficient together with EC50 when showing dose-responses.*

We have added Hill coefficients for all the fits.

> *(2) In Figure 1 (E, F), it might be clearer to use Venn-diagram to show whether there is overlapping among rapamycin-, menthol-, and cinnamaldehyde-responsive neurons. According to the authors' explanation, we can predict that rapamycin-insensitive, menthol-sensitive neurons should predominantly be cinnamaldehyde-responsive.*

Thank you for your suggestion. In these experiments, we applied several agonists and the combination of them would result in a visually crowded Venn diagram difficult to interpret. However, we agree, with the reviewer's suggestion, and discuss the percentage of the cinnamaldehyde+ neurons in the rapa- menthol+ population in *Trpm8*$^{-/-}$ neurons.

> *(3) In Figure 3(C), since F847 does not respond to either menthol or rapamycin, it should be excluded from (B). Otherwise it is misleading.*

Thank you for pointing this out. To clarify, we have included a calcium imaging trace for the F847 mutant, demonstrating a clear response to rapamycin in FigureS9. This additional data highlights that F847 does respond to rapamycin, albeit with a more modest response amplitude. This is now also clarified in the results section.

> *(4) The word "potency" in pharmacology usually refers to a smaller EC50 number in dose-dependent experiments. In "Effect of rapamycin analogs on TRPM8" session, the authors use "potency" to refer to response to a single-dose experiment of different compounds. The experiment does not measure potency.*

Thank you for pointing out this mistake. We have corrected the text and replaced "potency" with "efficacy".

> *(5) "2-methoxyl-" is misspelled in the text body.*

We have corrected the typo.

> *(6) It will be nice to include "vehicle" in Figure 6B, or alternatively normalize all individual traces to vehicle. In Figure 6C and D, everolimus has almost no effect with compared to vehicle, and should not be shown as if it had ~8% in Figure 6B.*

We have added the vehicle values to Figure 6B from the same experiments.

> ***Reviewer #3 (Recommendations For The Authors):***
>
> *(1) The NMR method presented here as novel and employed to identify a proposed molecule bound to a membrane protein (TRPM8 in this case) is not well explained and presented. Since several spectra need to be subtracted, the authors should present the raw data and the results of the subtractions step by step. Also, it seems that the height of the peaks in each spectra will be highly variable and thus a reliable criterion employed to scale spectra before subtraction. None of these problems are discussed of described.*

The reviewer is right, that the data transparency should be improved and due to the high molecular complexity of the samples the size of the STD effects should be carefully scaled. We carried out additional experimental replicas on new samples and addressed the inherent sample/peak height variability by rescaling the STD effects based on reference ^{1}H measurements. We provided supplementary spectra of the reference experiments without saturation (Figure S5) and the computed STTD spectra from three parallel NMR sessions (Figure S6). We changed panel C of Figure 2 in the main text and provided all the STD and the computed STDD and STTD spectra recorded on one set of NMR experiments. We added the

following paragraph to the main text: “To address the effect of the inherent variability of cellular samples on peak heights, STD effects were normalized based on the comparison of independent ^{1}H experiments (Figure S5). Three STTD replicates were computed, unambiguously confirming direct binding to TRPM8 in two datasets (Figure S6 A,B)”.

> *Importantly since this signal subtraction method is proposed as a new development, control experiments employing well-established pairs of ligand and membrane protein receptor should be performed to demonstrate the reliability of the method.*

We agree with the reviewer, that the STTD experiment as a new development needs further validation, however, this paper is a preliminary demonstration of a new strategy building on the well-established STD and STDD NMR methodologies. Our group is actively engaged in studying additional biological samples to enhance our understanding of the applicability of STTD NMR. These efforts also aim to address challenges such as sample and spectral complexity by refining and standardizing the proposed workflow.

> *(2) The tail currents shown in supplementary figure 3 are clearly not monoexponential. The fit to a single exponential can be seen to be inadequate and thus the comparison of kinetics of control, rapamycin and menthol is incorrect. At least two exponentials should be fitted and their values compared.*

We agree that the decay in the (combined) presence of agonists deviates from a simple monoexponential behavior. While we agree that fitting with two (or more) exponentials would provide a better fit, this also comes with greater variations/uncertainties in the fit parameters. This is particularly the case when inactivation is very slow and incomplete, or when the difference between slow and fast exponential time constants is <5, as seen with rapamycin and rapamycin +menthol. Therefore, we decided to provide monoexponential time constants as a proxy to describe the clear slowing down of activation and deactivation time courses in the presence of Type I agonists.

> *Also related to this aspect, recordings of TRPM8 currents can not be leak subtracted with a p/n protocol, thus a large fraction of the initial tail current must be the capacitive transient. There is no indication in the methods of how was this dealt with for the fitting of tail currents.*

As explained in the methods, capacitive transients and series resistance were maximally compensated. Therefore, we do not agree that a large fraction of the initial tail current must be capacitive. This can also be clearly seen in experiment such as Figure 1C, where the inward tail current is fully abolished in the presence of a TRPM8 antagonist. Likewise, very small and rapidly inactivating tail currents can be seen during voltage steps under control conditions (e.g. Figure S7 and S8 in the revised version).

> *(3) The docking procedure employed, as the authors show, is not appropriate for membrane proteins since it does not include a lipid membrane. It is not clear in the methods section if the MD minimization described applies only to the rapamycin molecule or to rapamycin bound to TRPM8.*
>
> *It is also not clear if the important residue Q861 (and other residues that are identified as interacting with rapamycin) were identified from dockings or proposed based on other evidence.*
>
> *(4) Identifying amino acid residues that diminish the response to a ligand, does not uniquely imply that they form a binding site or even interact with said ligand. It is entirely possible that they can be involved in the allosteric networks involved in the*

> *activating conformational change. This caveat should be clearly posited by the authors when discussing their results.*

In our study, we identified several residues that significantly reduce the response to rapamycin when mutated, while retaining robust responses to menthol, which indicates that these mutations do not affect crucial conformational changes leading to channel gating. While our cumulative data suggest that these residues may be involved in direct interaction with rapamycin, we recognize the alternative possibility that they allosterically affect rapamycin-induced channel gating. This is now clearly stated in the first paragraph of the discussion.

https://doi.org/10.7554/eLife.97341.2.sa0